Electrical Capacitance Volume Tomography

L.S. Fan

Department of Chemical and Biomolecular Engineering

April 23, 2009

Intrusive Techniques

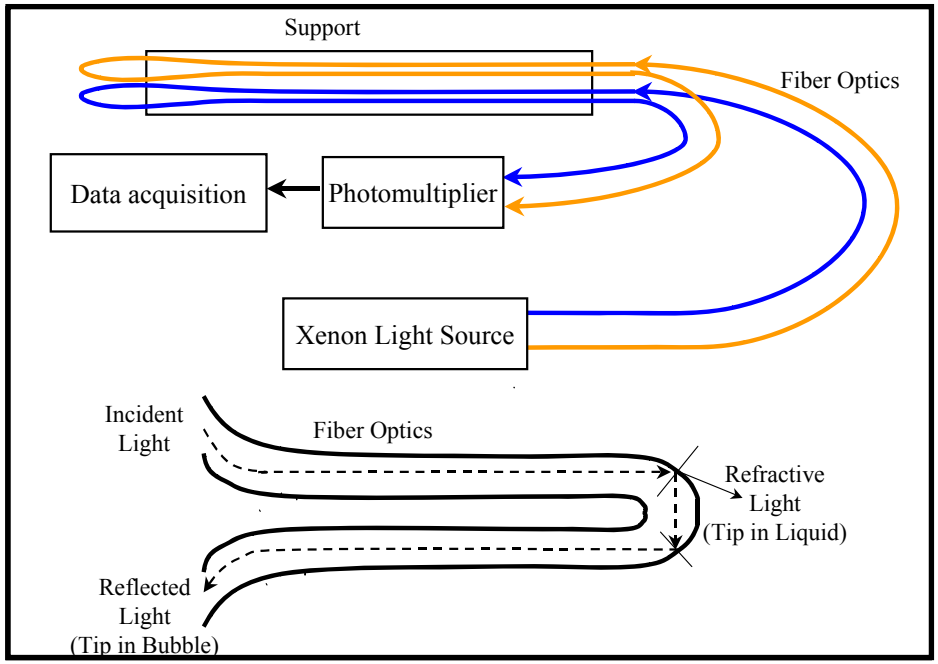

Optical Fiber Probe

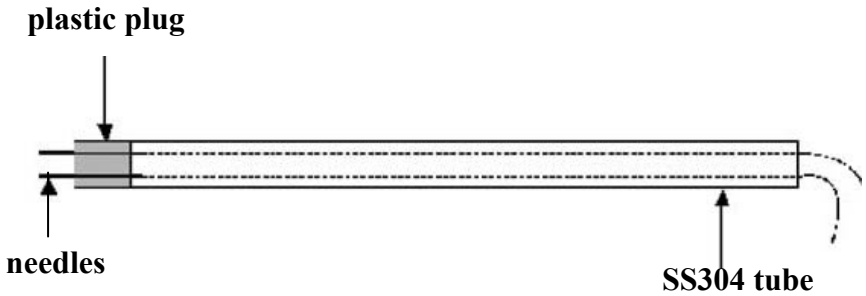

Conductivity Probe

(from Briens and Ellis, 2005)

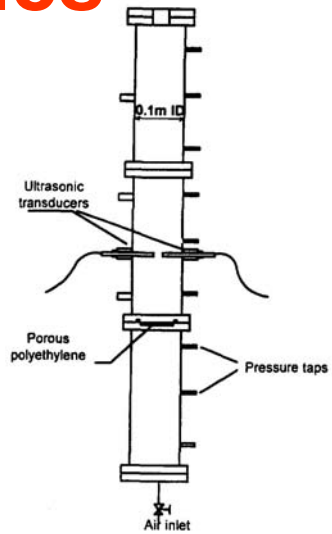

Ultrasound Probe

(from Stolojanu and Prakash, 1997)

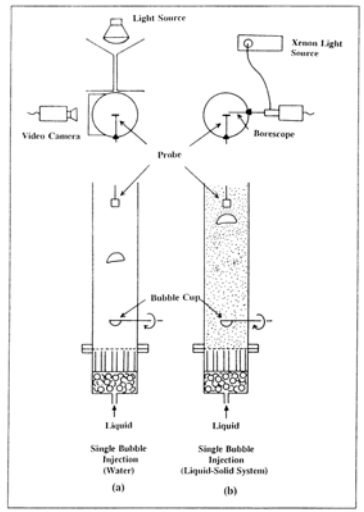

Figure 2. Experimental conditions.

Endoscopic Probe

(from Kumar et al., 1992)

Non-Intrusive Techniques

PIV (Particle Image Velocimetry)

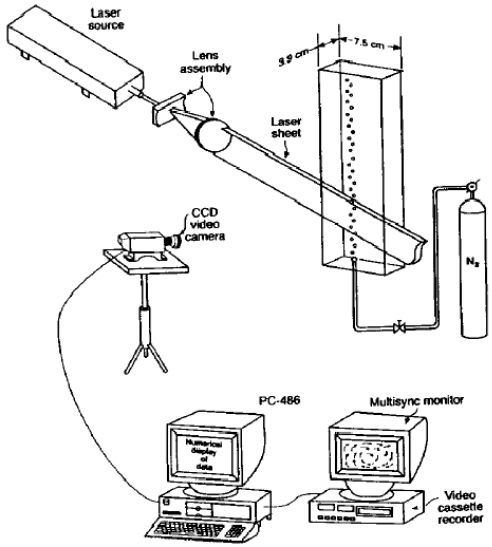

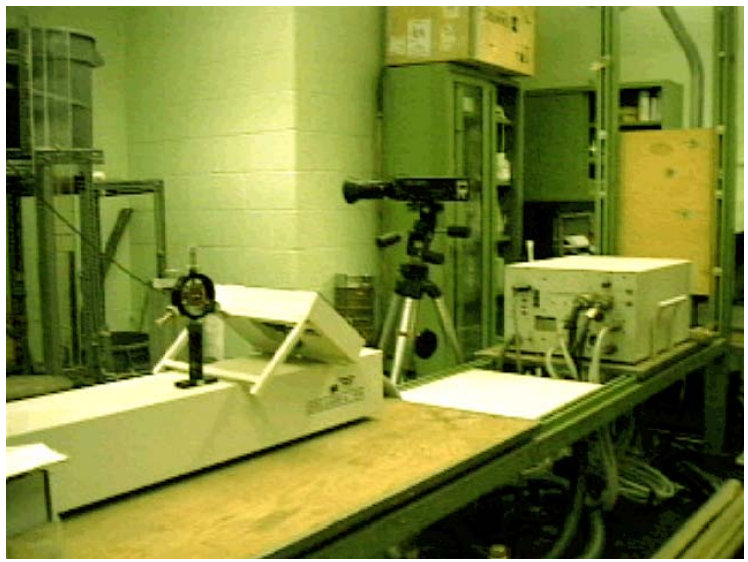

2D FiberFlow Optics/Transmitter LDV/PDPA System

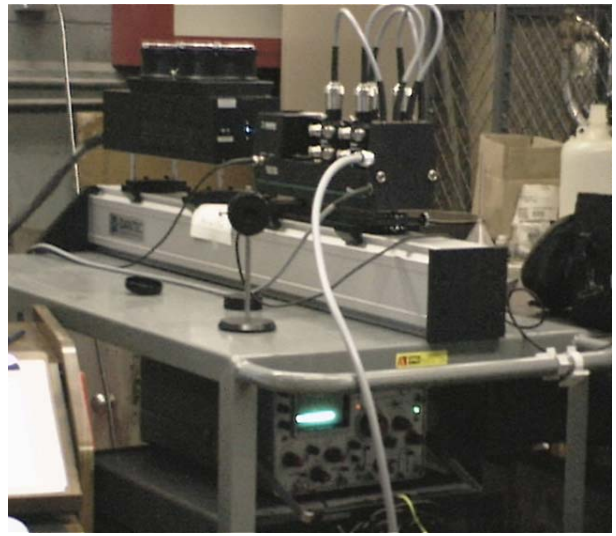

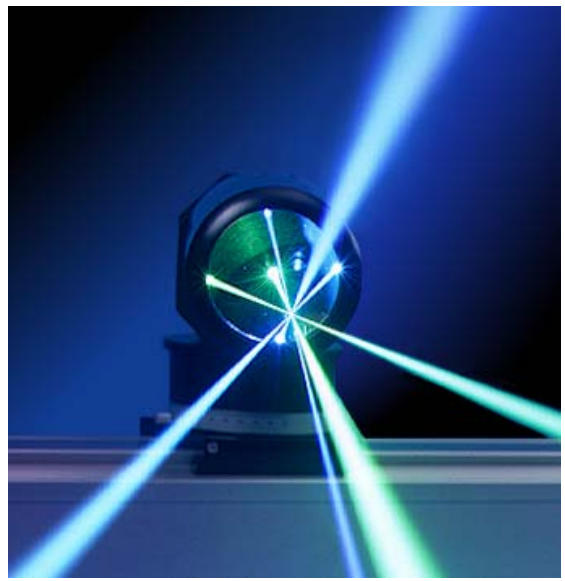

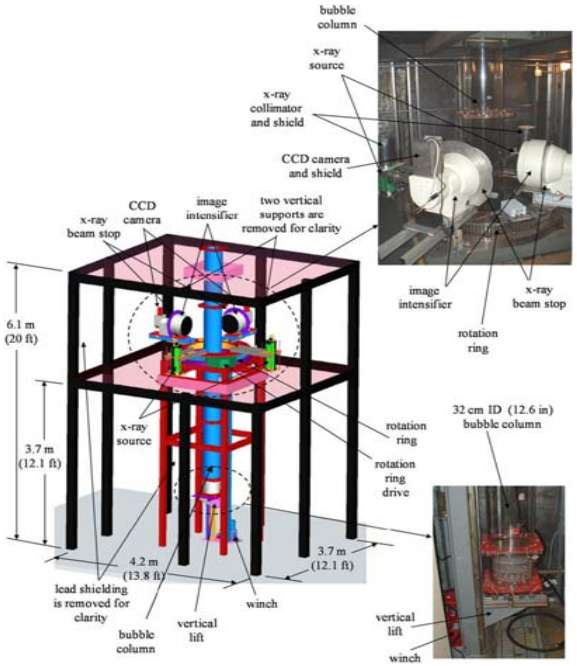

X-Ray Flow Visualization Facility (from Hubers et al., 2005)

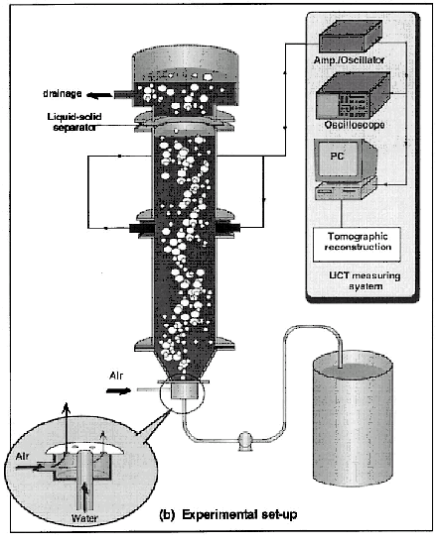

Ultrasonic tomography (from Warsito et al., 1999)

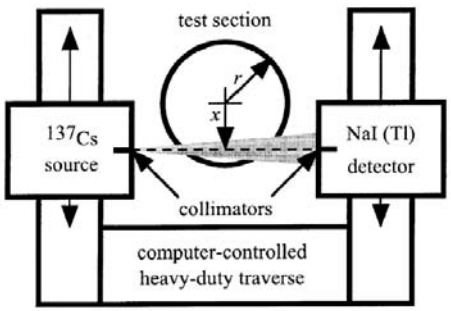

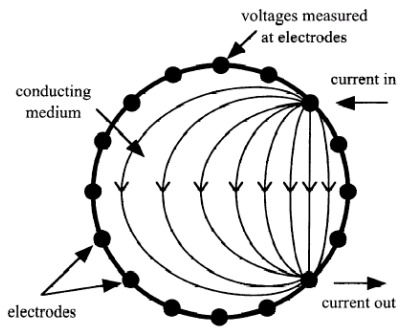

Gamma-Densitometry Tomography and Electrical-Impetence Tomography (George et al., 2001)

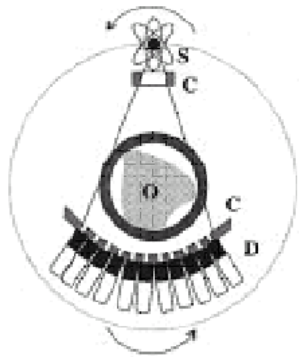

Computer Tomography (CT) (Chaouki et al., 1997)

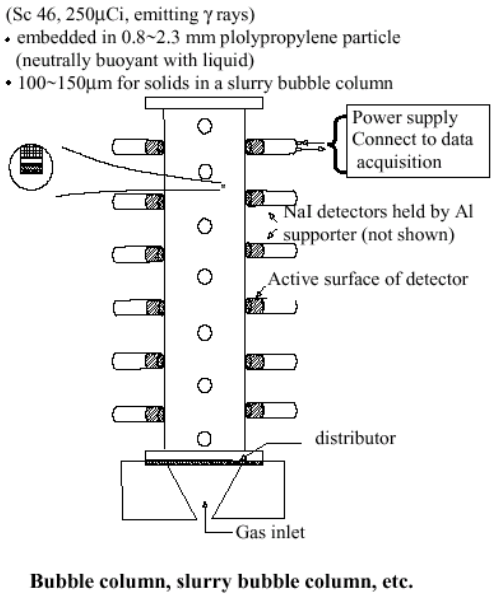

Computer-Automated Radioactive Particle Tracking (from Larachi et al., 1997)

Positron Emission Particle Tracking (from the University of Birmingham)

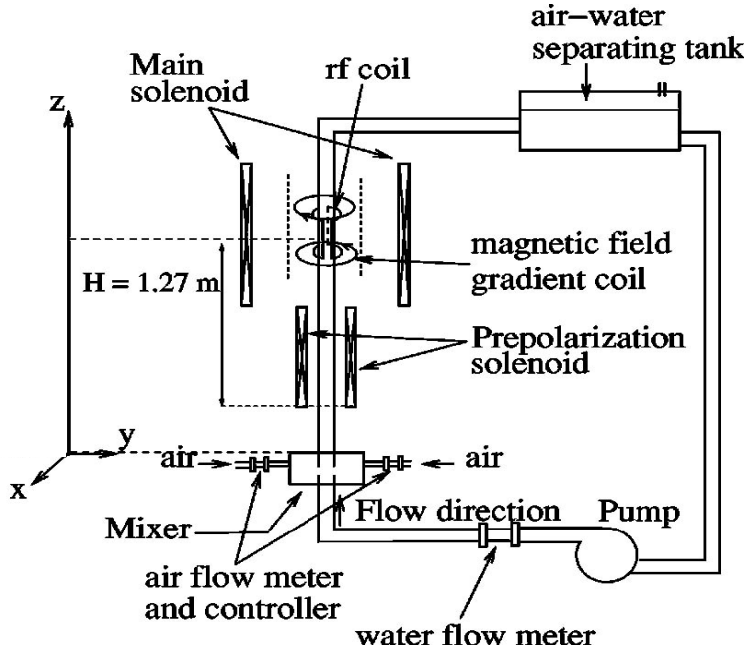

Nuclear Magnetic Resonance imaging (from Le Gall et al., 2001)

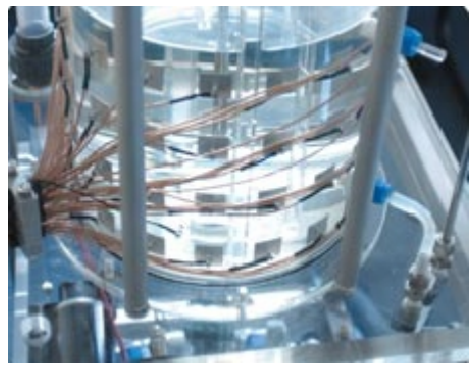

Electrical Impedance Tomography (from the University of Manchester)

Confocal Microscopy

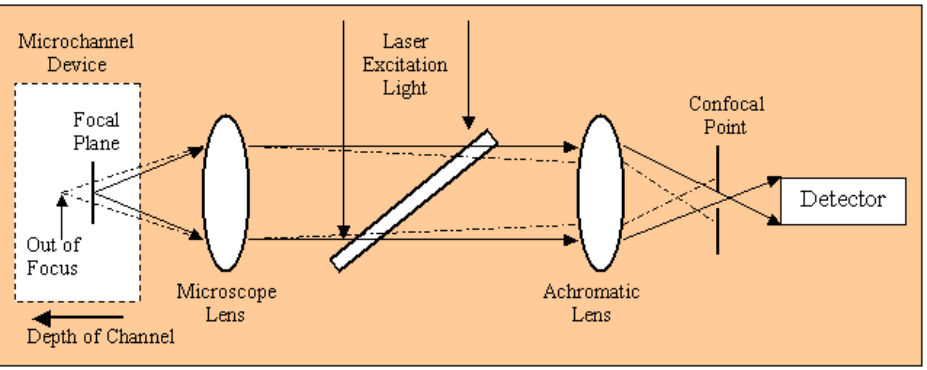

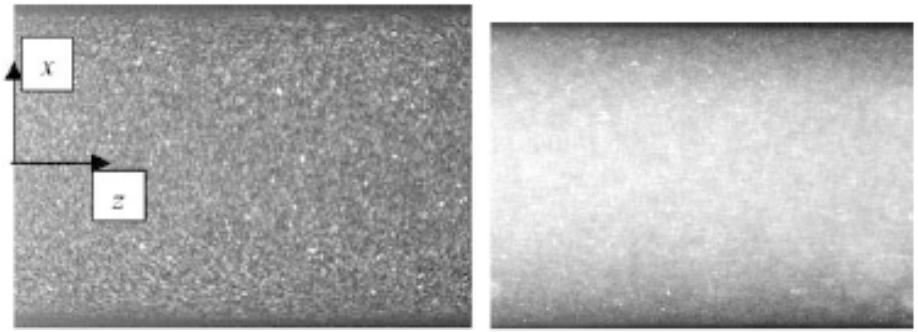

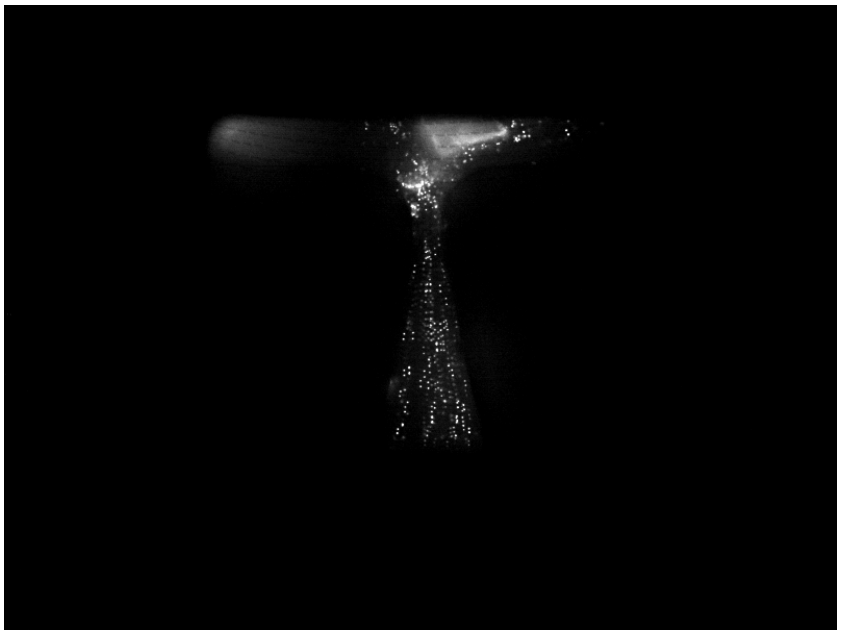

Tracer particles flowing through converging channel (100 μm down to 20 μm), imaged at 1000 frames per second.

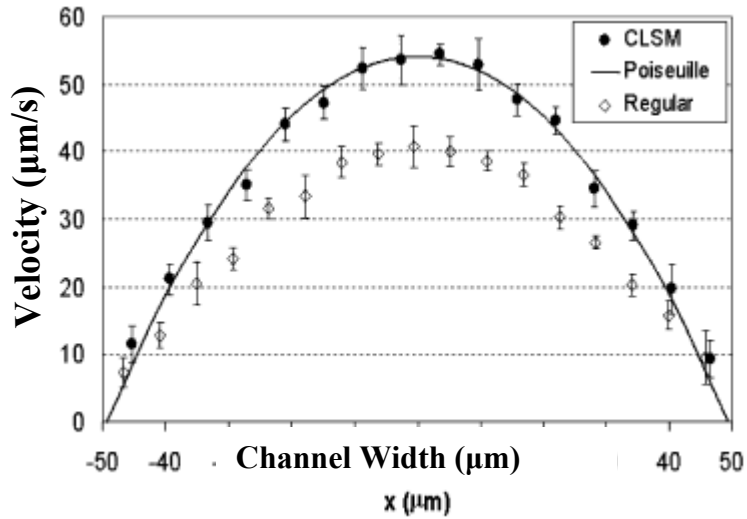

Velocity profile in middle depth of channel (ID=99μm)

[Park et al., Experiments in Fluids, 2004]

- Pioneering work on ECT in the 80’s at METC (G. Fasching, N. Smith, P. Nicoletti, J. Halow) and UMIST (M. Beck..)

- Most Active University Consortium on Various Types of Tomography in UK (Manchester, Leeds, Birmingham, Cambridge…)

ECT- Image Reconstruction

Image reconstruction:

$C_\theta(\Gamma)$ ⇒ Image

Measurement principle

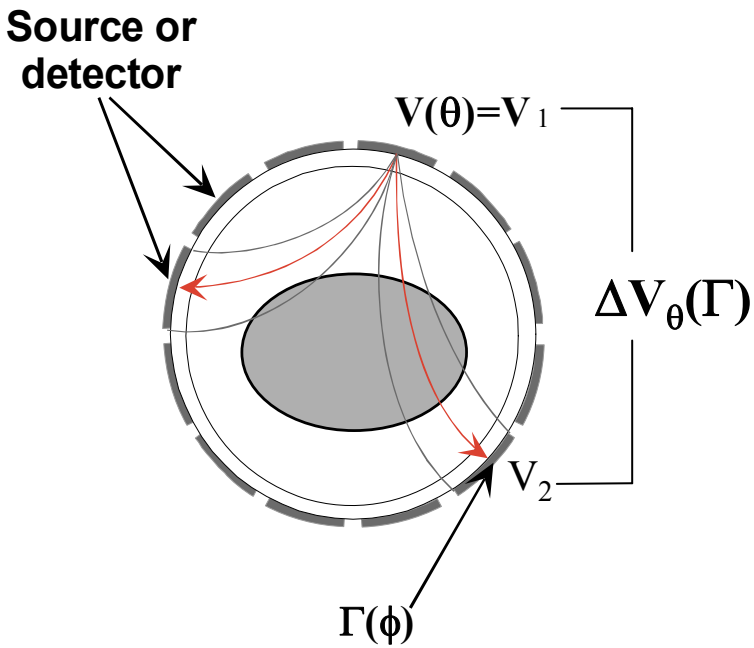

$$\nabla \cdot \varepsilon(\mathbf{r}) \nabla \phi(\mathbf{r}) = -\rho$$

$$C_\theta(\Gamma) = -\frac{1}{\Delta V_\theta(\Gamma)} \varepsilon_0 \oint_\Gamma \varepsilon(\mathbf{r}) \nabla \phi(\mathbf{r}) \, dl$$

Sensitivity model (linearization)

$$C = SG \qquad G = S^T C$$

S : Sensitivity Matrix

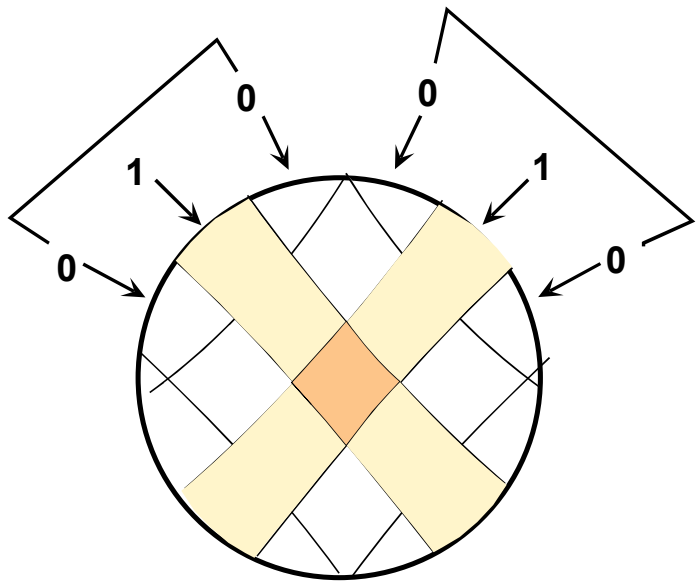

Linear Back Projection

ECVT - 3D Image digitization

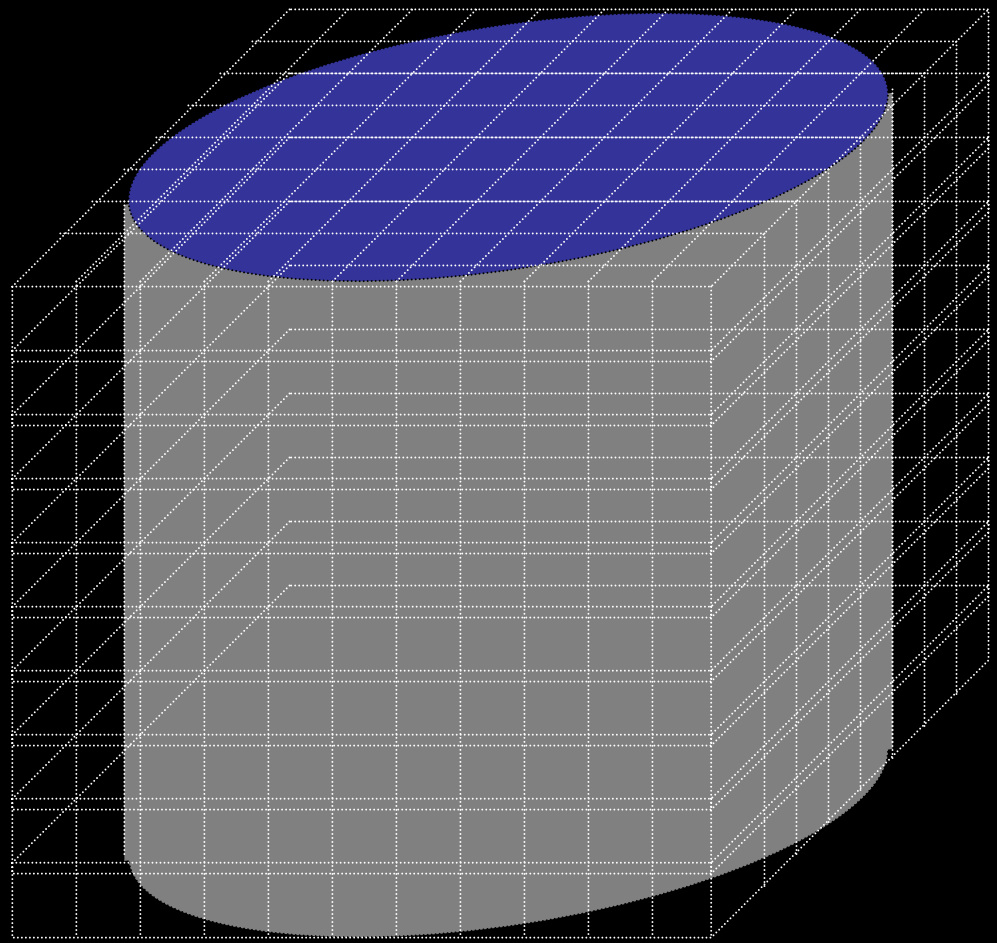

Volume image (voxel):

Digitization	Resolution
20X20X20	0.125 cm^3
32X32X32	0.0305 cm^3
64X64X64	3.81 mm^3
128X128X128	0.48 mm^3

ECVT - 3D Sensor Models

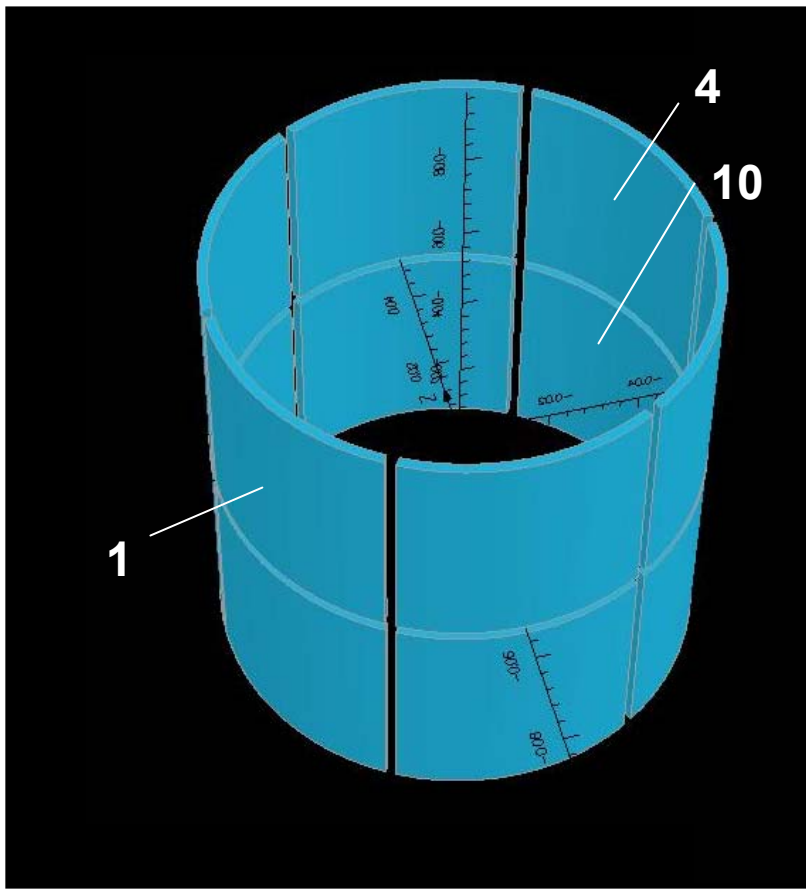

Model A
(Square shape)

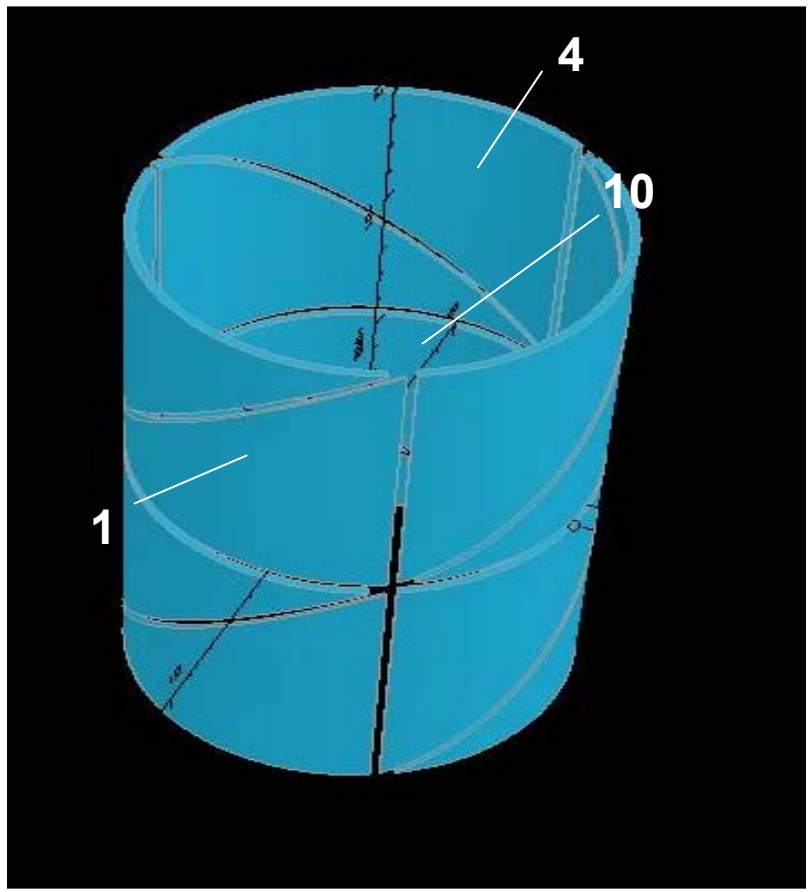

Model B
(Triangular shape)

3D-ECT sensor design concept

(Axial and lateral distribution of electrical field)

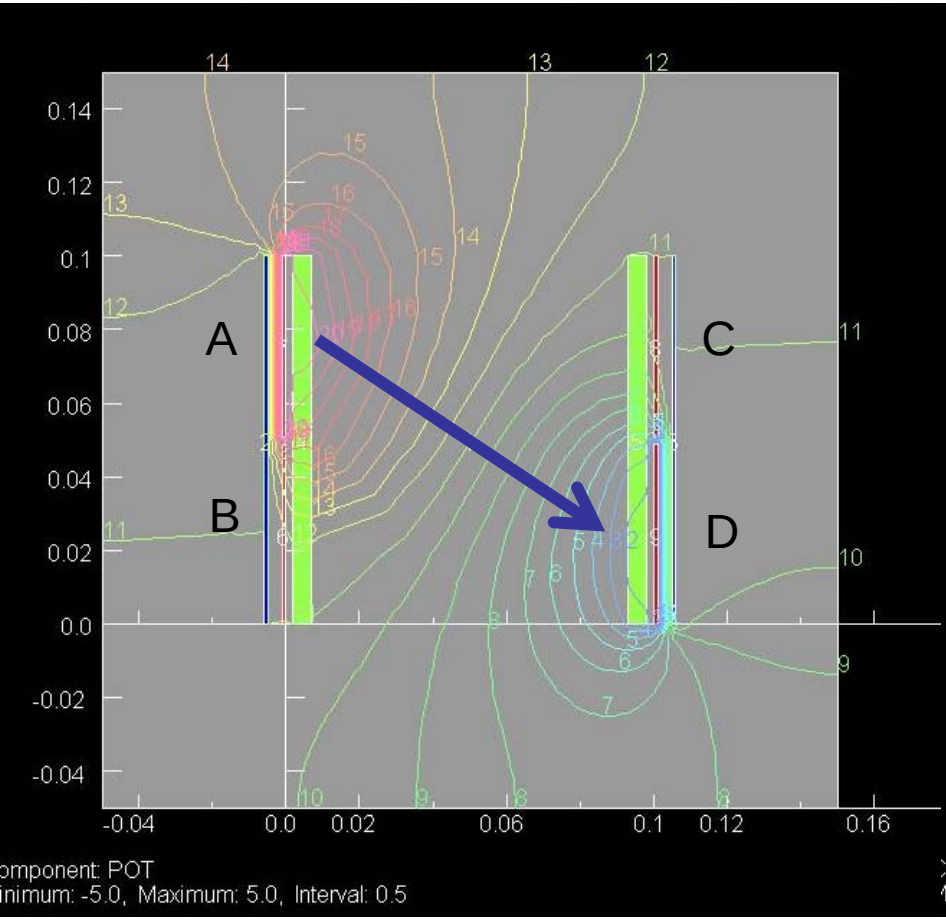

A-D pair

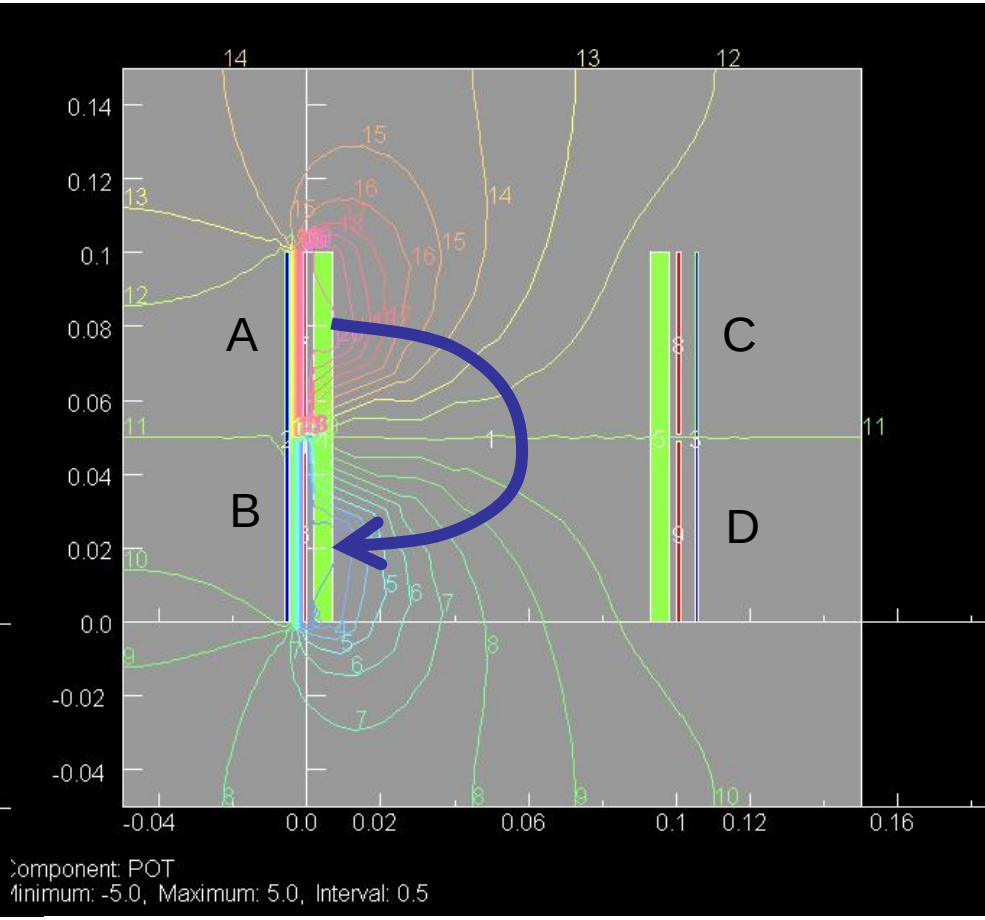

A-B pair

Basic schemes of ECT image reconstruction techniques

Technique	Description	References
Non-iterative techniques		
LBP (Linear Back Projection)	$G = S^T C$	Huang et al., 1989
SVD (Singular Value Decomposition)	$S = U\Sigma V^T \qquad S^{-1} = V\Sigma^{-1}U^T$	Yang et al., 2003
TR (Thikonov Regularization)	$G = \left(S^T S + \mu I\right)^{-1} S^T C$	Peng et al., 2000
Iterative techniques		
ART/SIRT	$G^{(k+1)} = G^{(k)} + \alpha^{(k)} S^T \left[C - C^*\left(G^{(k)}\right)\right]$	
	$\alpha^K = \frac{2}{\lambda_{\max}}$ $C^*\left(G^K\right) = SG^K$	
Optimization	$\nabla f \to 0$	

Comparisons of 2D reconstructed results (noisy data)

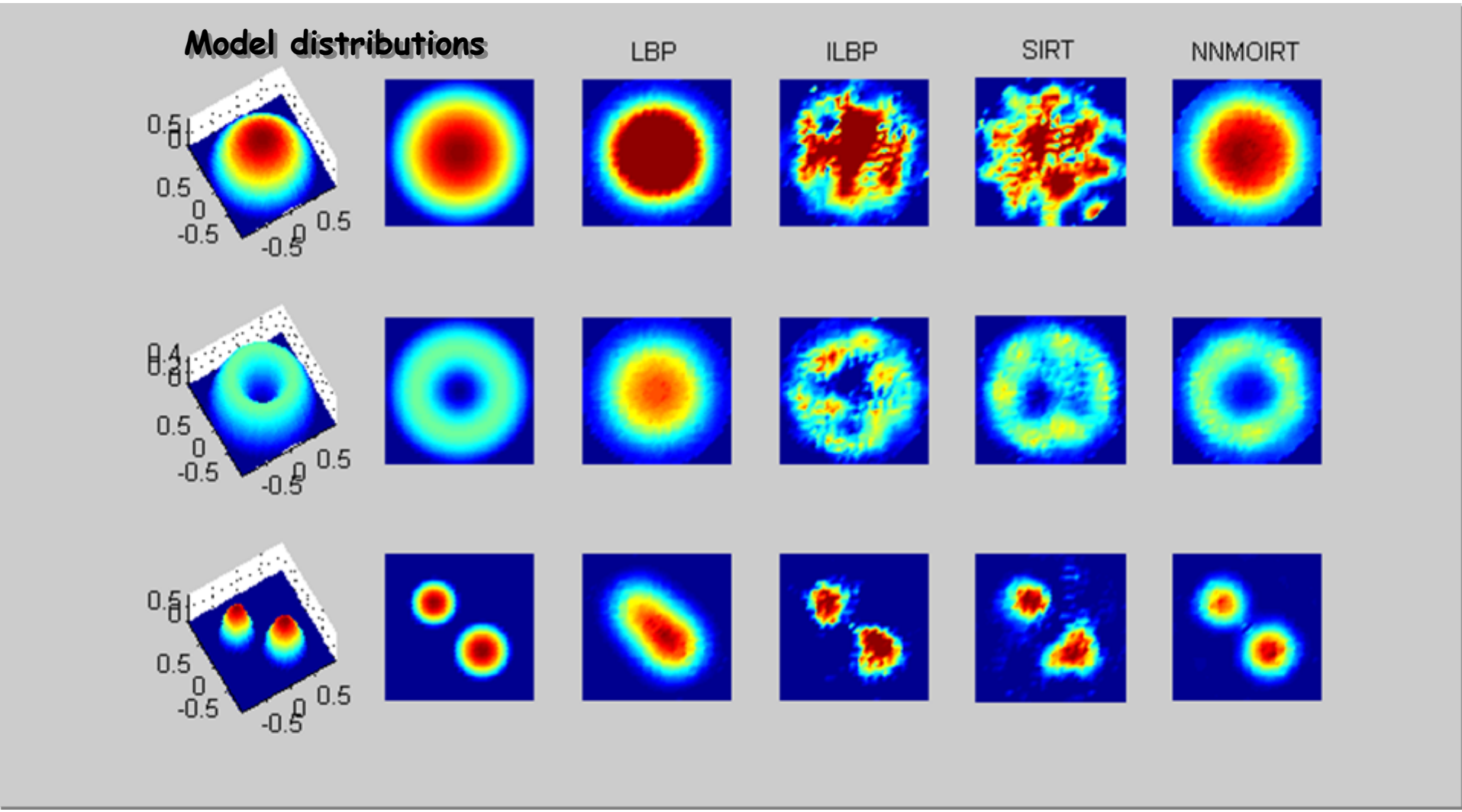

NN-MOIRT algorithm

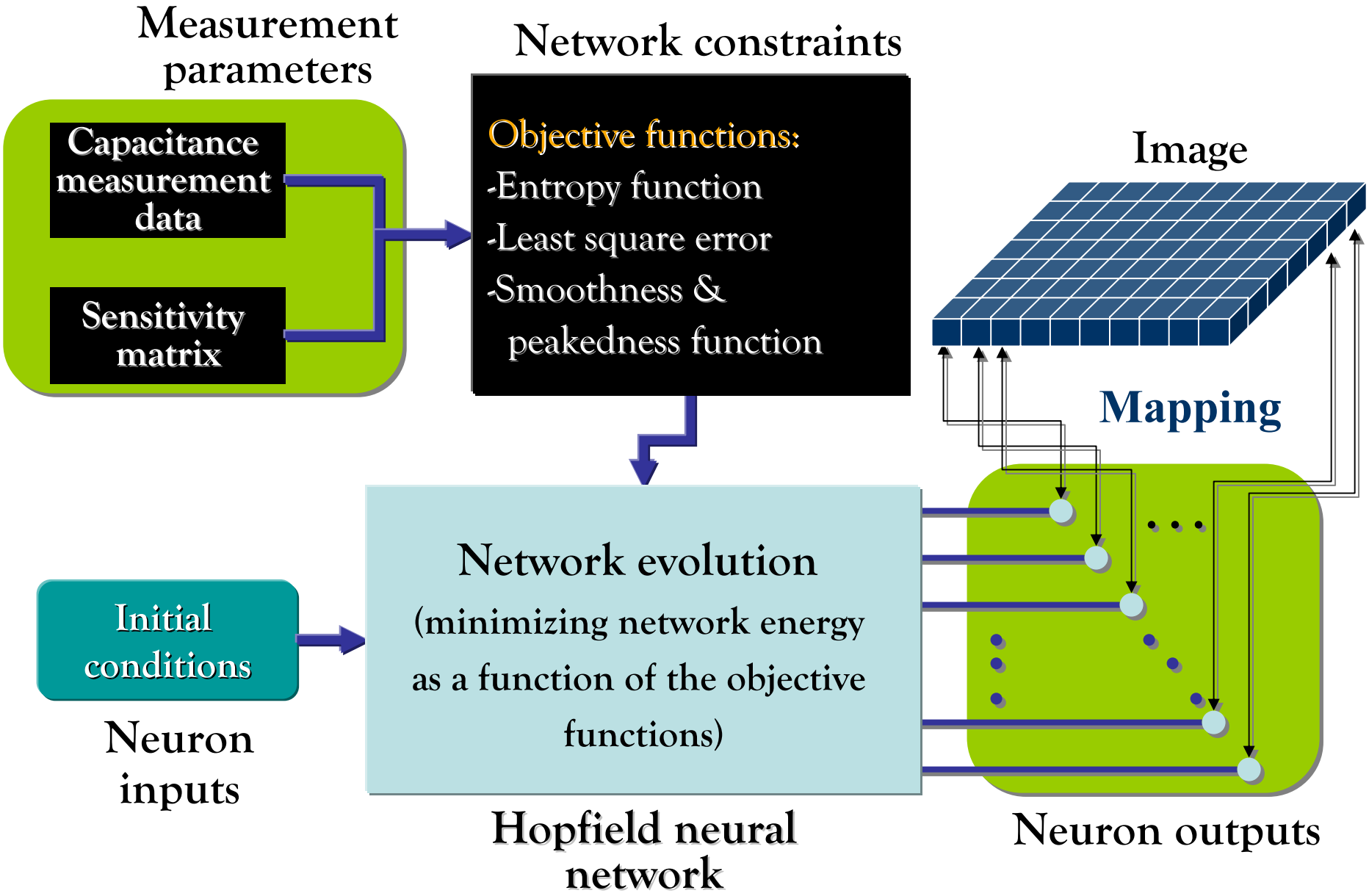

Objective functions

Negative entropy function $f_1(\mathbf{G}) = \gamma_1 \sum_{j=1}^{N} G_j \ln G_j$

Error function $f_2(\mathbf{G}) = \frac{1}{2}\gamma_2 \left\| \mathbf{SG} - \mathbf{C} \right\|^2 = \gamma_2 \sum_{i=1}^{M} \left(\sum_{j=1}^{N} S_{ij} G_j - C_i \right)^2$

3-D Smoothness function $f_3(\mathbf{G}) = \frac{1}{2}\gamma_3 \left(\mathbf{G}^T \mathbf{XG} + \mathbf{G}^T \mathbf{G} \right)$

3-to-2D and 3-to-1D matching function for 3-D imaging

$$f_4(\mathbf{G}) = \frac{1}{2}\gamma_4 \left\{ \left\| \mathbf{H}^1 \mathbf{G} - \mathbf{G}_{2D}^1 \right\|^2 + \left\| \mathbf{H}^2 \mathbf{G} - \mathbf{G}_{2D}^2 \right\|^2 \right\}$$

$$= \frac{1}{2}\gamma_4 \left\{ \sum_{j=1}^{N_{1D}} \left(\sum_{k=1}^{N} H_{jk}^1 G_k - G_{1D,j} \right)^2 + \sum_{j=1}^{N_{2D}} \left(\sum_{k=1}^{N} H_{jk}^2 G_k - G_{2D,j} \right)^2 \right\}$$

Modified Hopfield Network Energy E

$$E(\mathbf{G}) = \sum_{i}^{4} w_i f_i(\mathbf{G}) + \sum_{k=1}^{3}\sum_{i=1}^{M_k} \Psi\left(z_i^k\right) + \sum_{j=1}^{N} \frac{1}{R_j} \int_0^{G_j} f_\Sigma^{-1}(G)\,dG$$

$$z_i^1 = \sum\nolimits_j^N S_{ij} G_j - C_i \qquad z_i^2 = \sum\nolimits_{j=1}^N H_{ij}^1 G_j - G_{1D,i} \qquad z_i^3 = \sum\nolimits_{j=1}^N H_{ij}^2 G_j - G_{2D,i}$$

$$\frac{d\Psi}{dz_i^k} = \delta\left(z_i^k\right) = \begin{cases} 0 & \text{if } z_i^k \le 0 \\ \alpha^k z_i^k & \text{if } z_i^k > 0 \end{cases} \qquad (k = 1,2,3)$$

Network evolution

$$\mathbf{u}'(t) = -\frac{\mathbf{u}(t)}{\tau} - \left[\frac{w_1\gamma_1}{C_0}\left\{\mathbf{1} + \ln \mathbf{G}(t)\right\} + \frac{w_2\gamma_2}{C_0}\mathbf{S}^T\left\{\mathbf{S}\mathbf{G}(t) - \mathbf{C}^1\right\} + \frac{w_3\gamma_3}{C_0}\left\{\mathbf{X}\mathbf{G}(t) + \mathbf{G}(t)\right\}\right.$$

$$+ \frac{w_4\gamma_4}{C_0}\left(\mathbf{H}^{1T}\left\{\mathbf{H}^1\mathbf{G}(t) - \mathbf{G}_{1D}\right\} + \mathbf{H}^{2T}\left\{\mathbf{H}\mathbf{G}(t) - \mathbf{G}_{2D}\right\}\right)$$

$$\left. + \mathbf{S}^{1T}\delta\left[\mathbf{S}\mathbf{G}(t) - \mathbf{C}^1\right] + \mathbf{H}^{1T}\delta\left[\mathbf{H}^1\mathbf{G}(t) - \mathbf{G}_{1D}\right] + \mathbf{H}^{2T}\delta\left[\mathbf{H}^2\mathbf{G}(t) - \mathbf{G}_{2D}\right]\right]$$

Hopfield Network

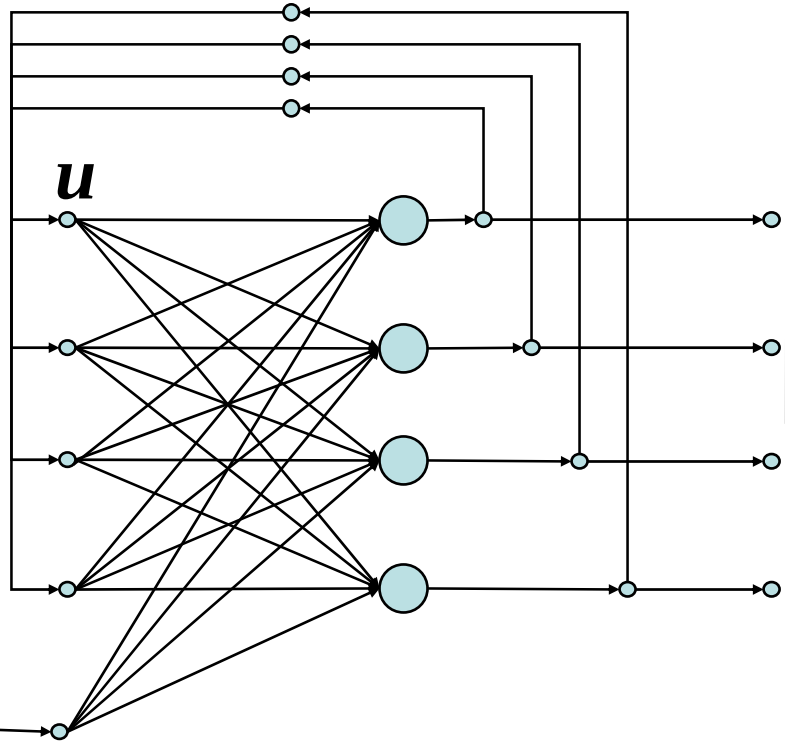

OUTPUTS v

$$v_j = f_\Sigma(u_j)$$

INPUTS
(Initial conditions)

$$\frac{dE(\mathbf{v})}{dt} = \sum_{j=1}^{N} \frac{\partial E(\mathbf{v})}{\partial v_j} \frac{dv_j}{dt} = -\sum_{j=1}^{N} C_{0j} \frac{du_j}{dt} \frac{dv_j}{dt}$$

$$C_{0j} \frac{du_j}{dt} = -\frac{\partial E(\mathbf{v})}{\partial v_j}$$

$$= -\sum_{j=1}^{N} C_{0j} \left[\frac{\partial f_\Sigma(u_j)}{\partial u_j} \right] \left(\frac{du_j}{dt} \right)^2 = -\sum_{j=1}^{N} C_{0j} \left[\frac{\partial f_\Sigma^{-1}(v_j)}{\partial v_j} \right] \left(\frac{dv_j}{dt} \right)^2$$

$$\frac{dE}{dt} \le 0; \frac{du_j}{dt} = \frac{dv_j}{dt} = 0, t \to \infty$$

Network evolution

$$\mathbf{u}'(t) = -\frac{1}{C_0}\nabla E(\mathbf{G}) = -\frac{\mathbf{u}(t)}{\tau} - \left[\omega_1\gamma\left(\mathbf{1}+\ln\mathbf{G}(t)\right)+\omega_2\gamma_2\mathbf{S}^T\mathbf{z}(t) + \omega_3\gamma_3\left(\mathbf{X}\mathbf{G}(t)+\mathbf{G}(t)\right)+\mathbf{S}^T\delta(\mathbf{z}(t))\right]$$

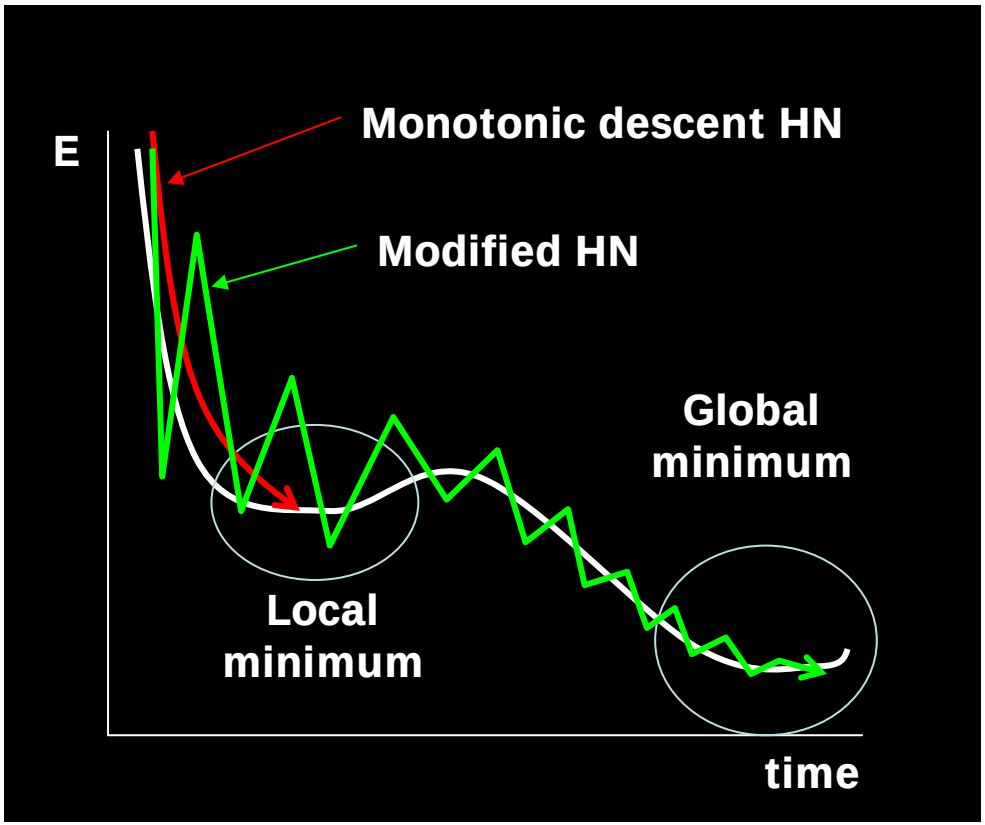

$$\nabla E(G) = \left[\frac{\partial E(G)}{\partial G_1}, \frac{\partial E(G)}{\partial G_2}, \cdots, \frac{\partial E(G)}{\partial G_N}\right]^T$$

$$u(t) = [u_1(t), u_2(t), \cdots, u_N(t)]^T$$

$$G(t) = [G_1(t), G_2(t), \cdots, G_N(t)]^T$$

$$z(t) = [z_1(t), z_2(t), \cdots, z_N(t)]^T$$

$$\frac{d\Psi}{dz_i} = \delta(z_i) = \begin{cases} 0 & \text{if } z_i \le 0 \\ \alpha z_i & \text{if } z_i > 0 \end{cases}$$

$$\alpha(t) = \alpha_0 + \varsigma\exp(-\eta t)$$

Flow structure in 4” and 12” fluidized beds with 60μm FCC particles

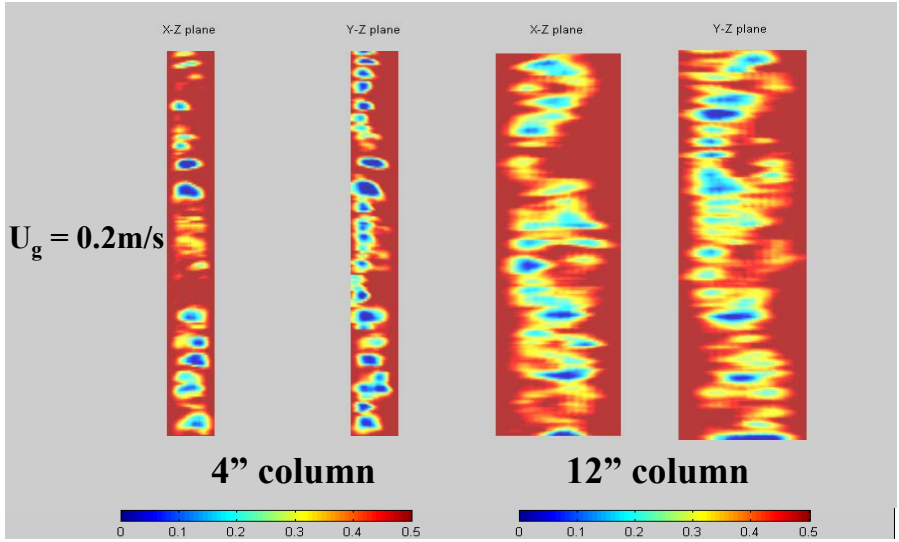

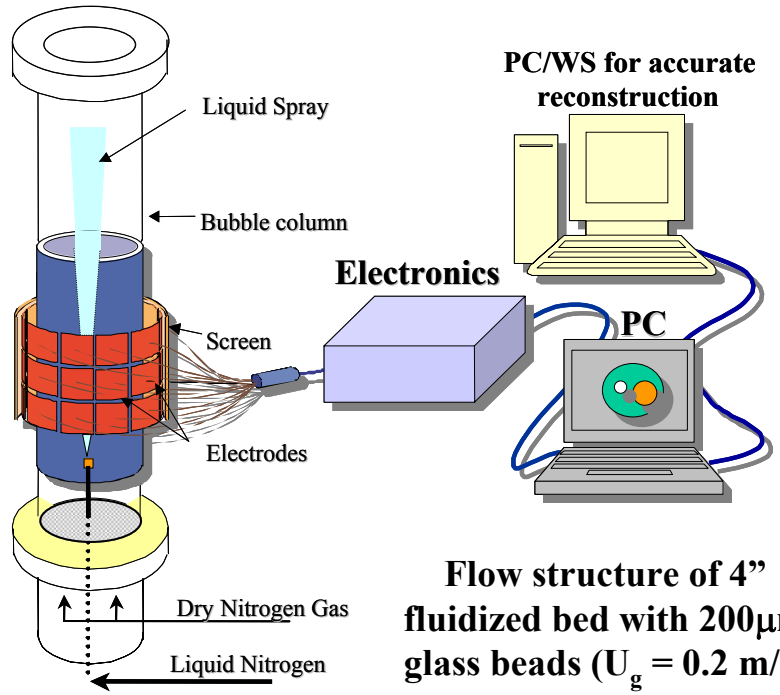

Flow structure of 4” fluidized bed with 200μm glass beads (U_g = 0.2 m/s)

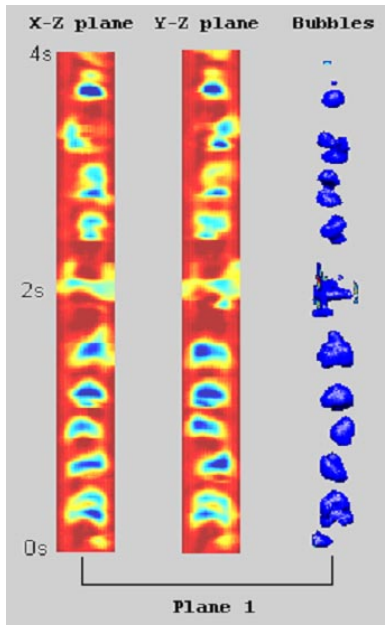

without liquid injection

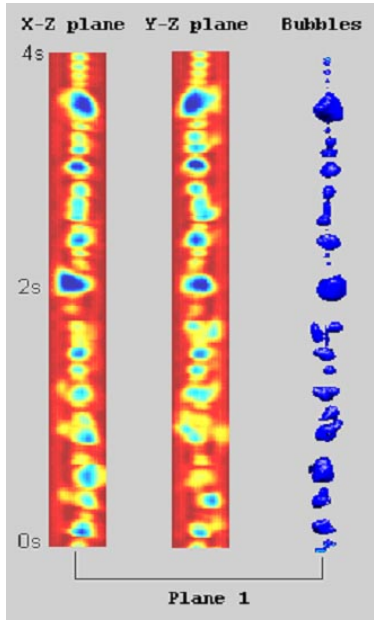

with liquid injection

Choking Phenomenon in Gas-Solid Circulating Fluidized Beds

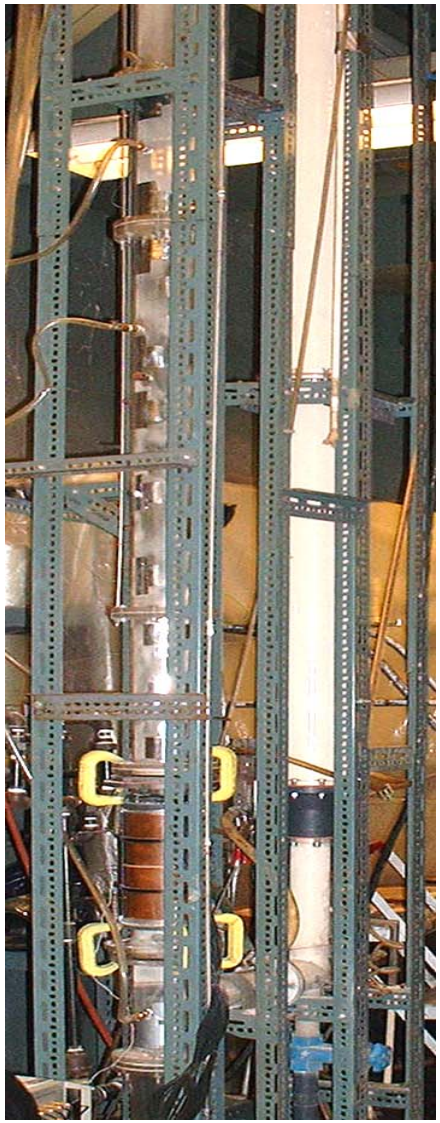

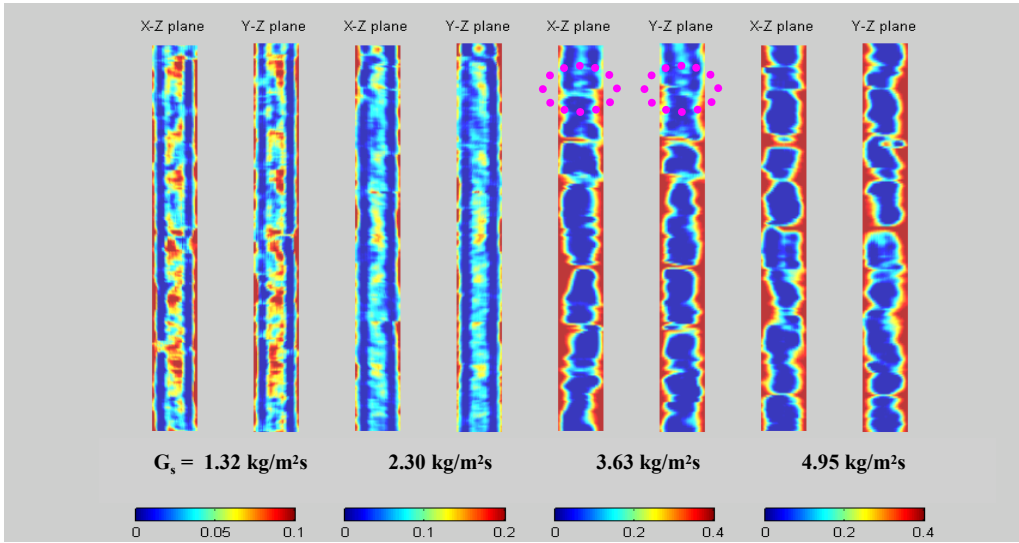

FCC catalyst (Group A)

d_p = 60 μm

ρ_p = 1450 kg/m³

U_g = 0.97 m/s

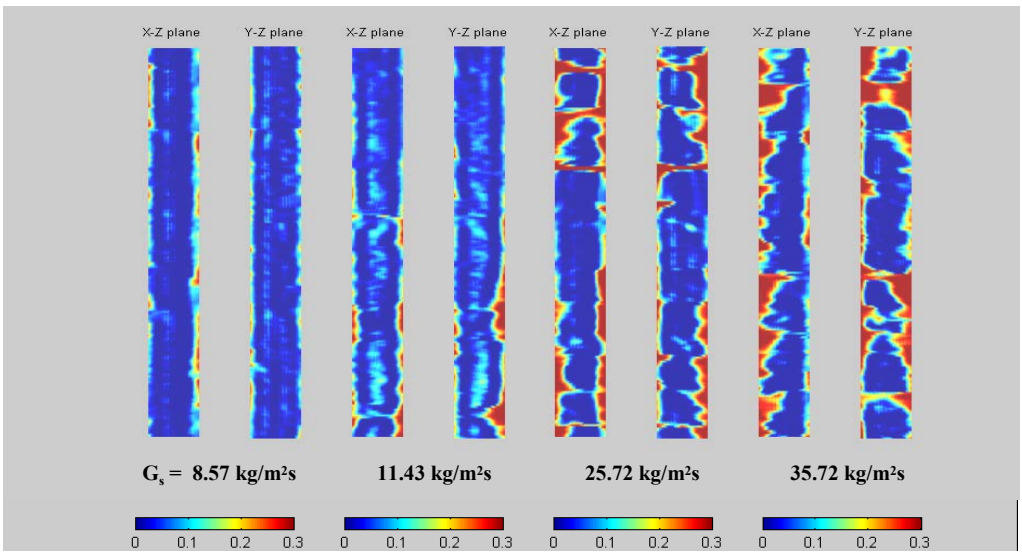

Sand particles (Group B)

d_p = 240 μm

ρ_p = 2200 kg/m³

U_g = 2.4 m/s

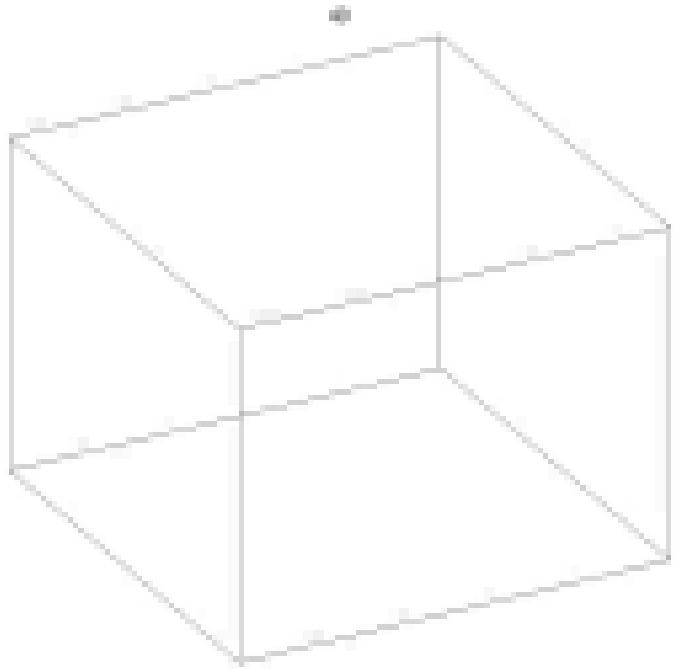

Real time 3D Imaging of a bubble in a 4" ID Fluidized Bed (GB 200,10cm/s)

360° Image

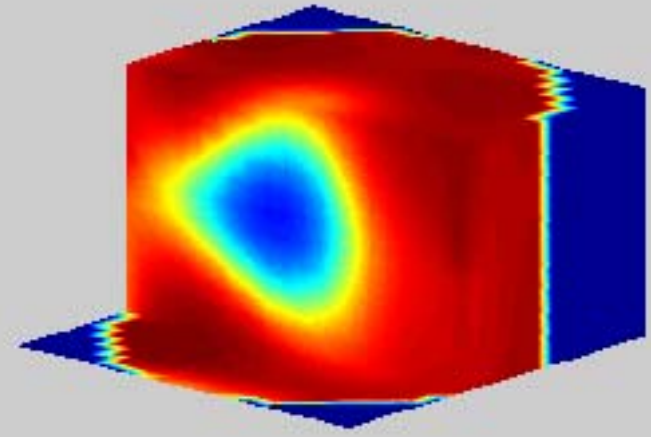

Solid concentration map

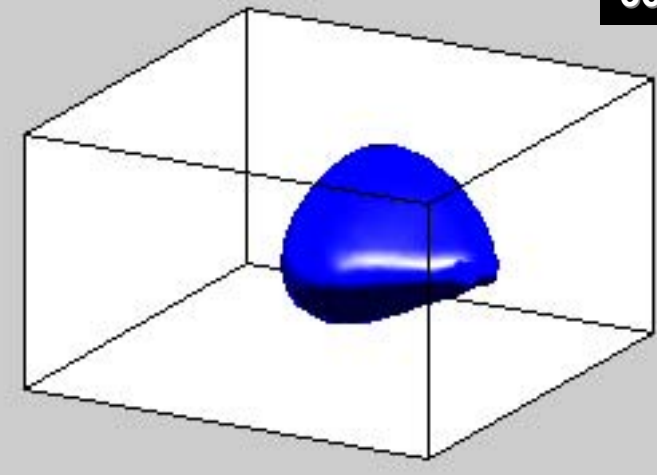

3D Image of Bubble

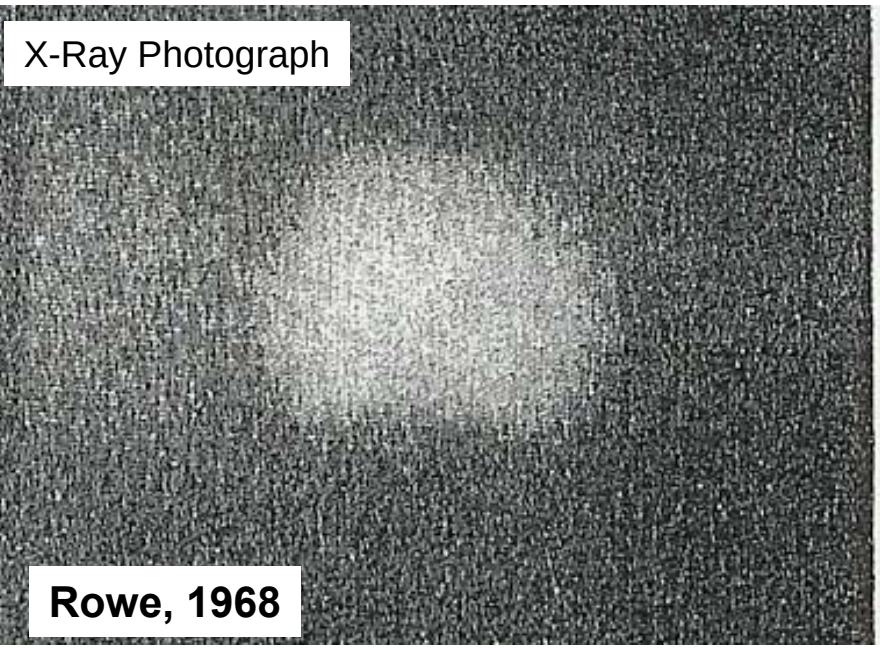

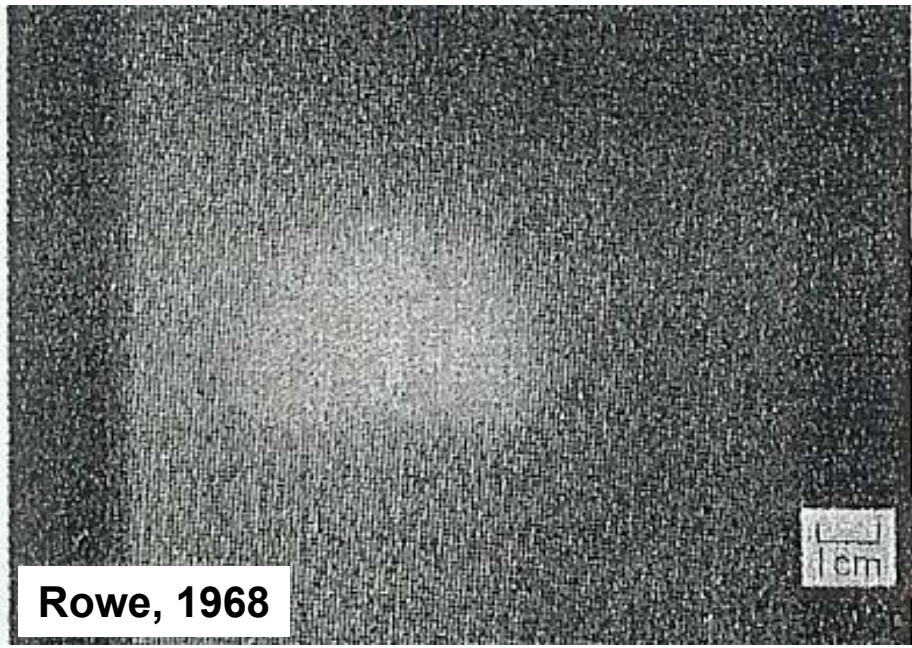

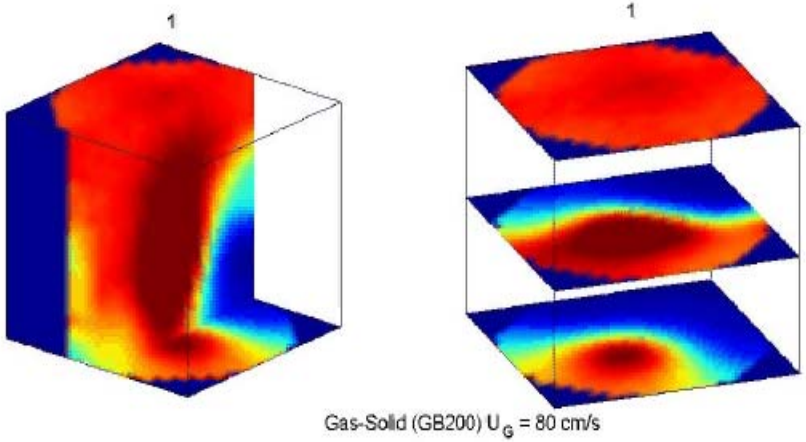

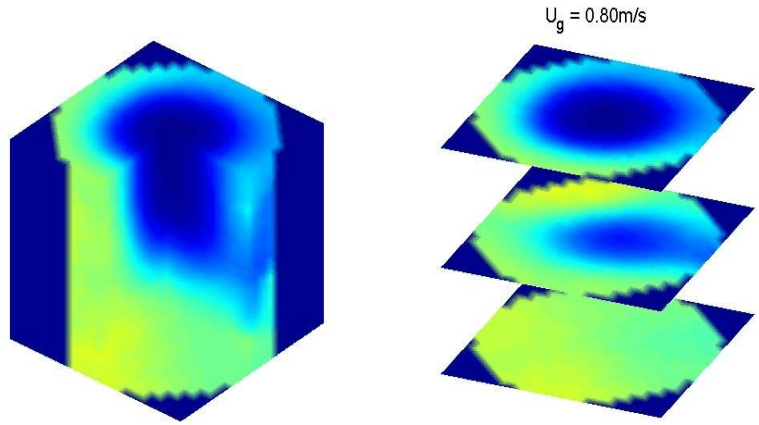

Real Time 3D Imaging of Gas-Solid Fluidized Bed with 200µm Glass Beads (Ug = 0.8 m/s)

Real Time 3D Imaging of Gas-Solid Fluidized Bed with 60µm FCC particles (Ug = 0.8 m/s)

Real time volume imaging of bubbly flow in G-L system (2)

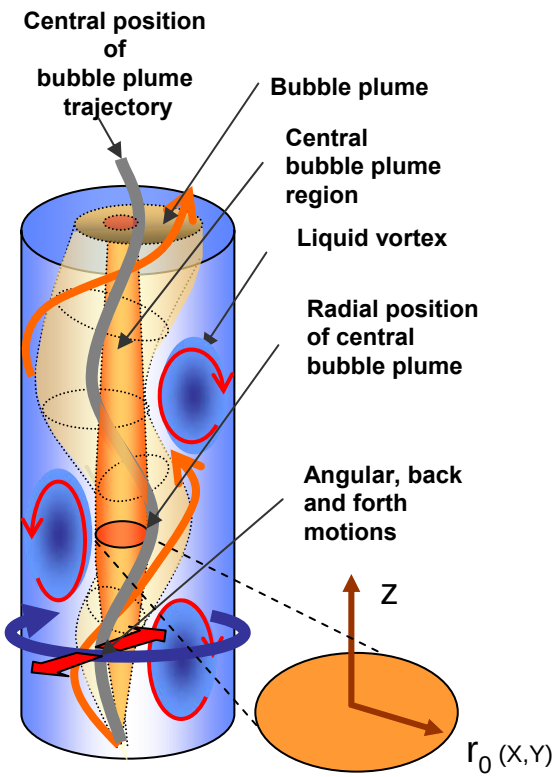

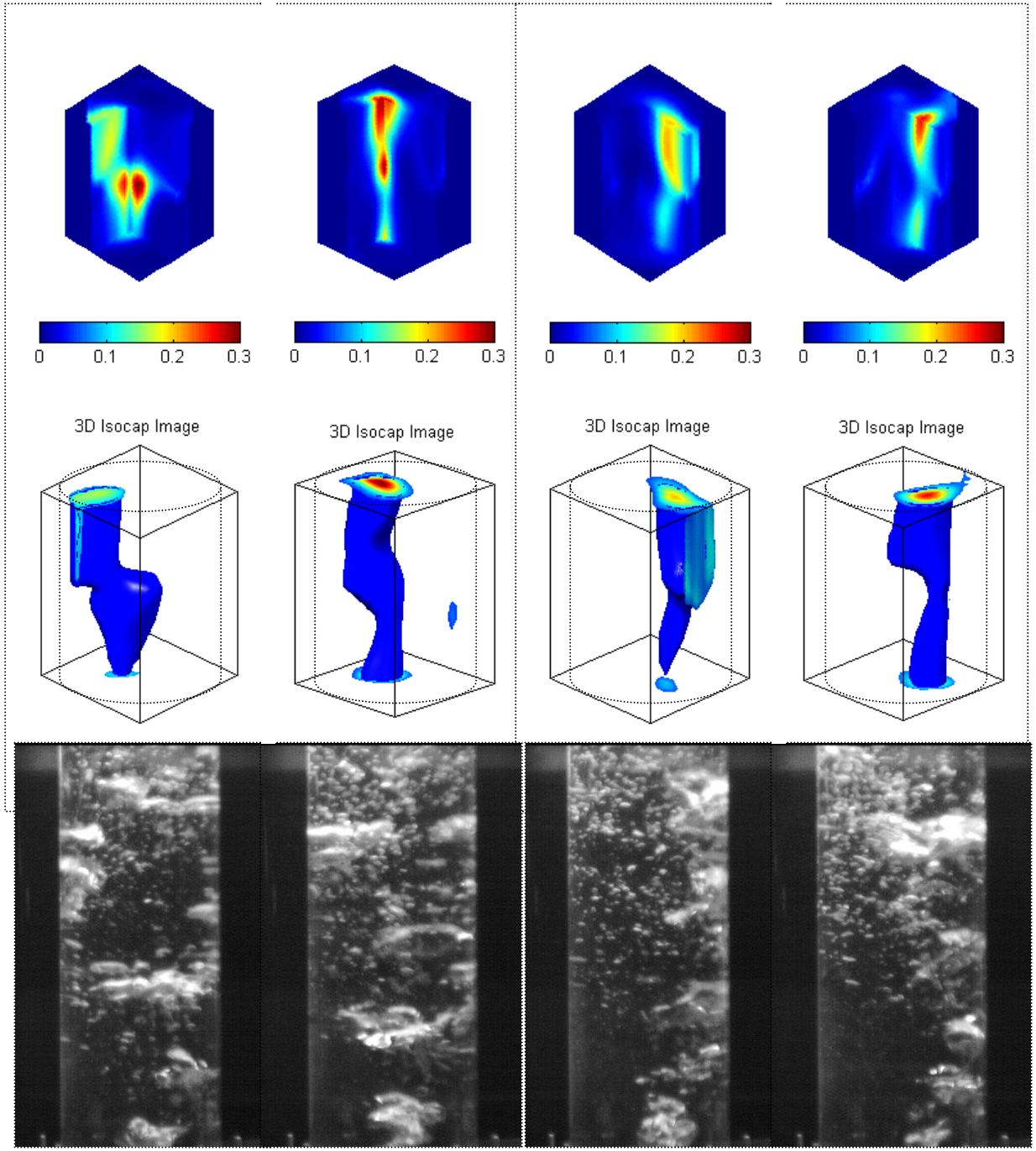

Sensors and Experimental Setup

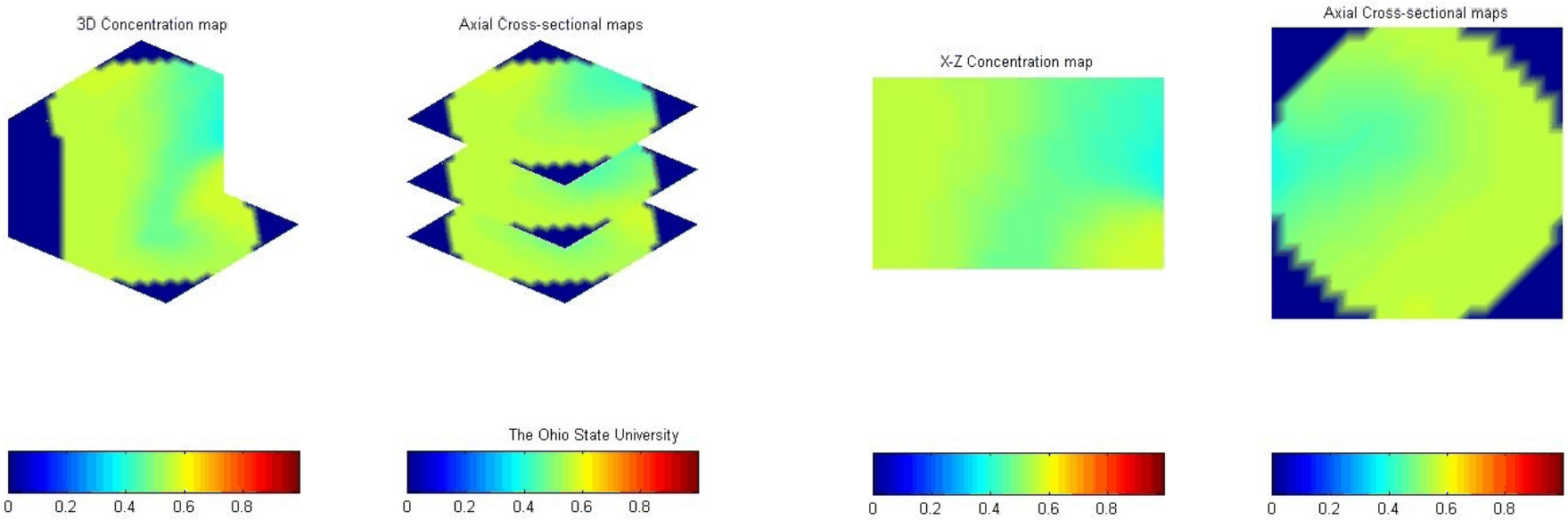

Superficial gas velocity: Ug=0.032 m/s; Side gas velocity: Ug_side=15.5 m/s; Side solids velocity: Us_side=0

Superficial gas velocity: Ug=0.032 m/s; Side gas velocity: Ug_side=16.3 m/s; Side solids velocity: Us_side=16.3 m/s

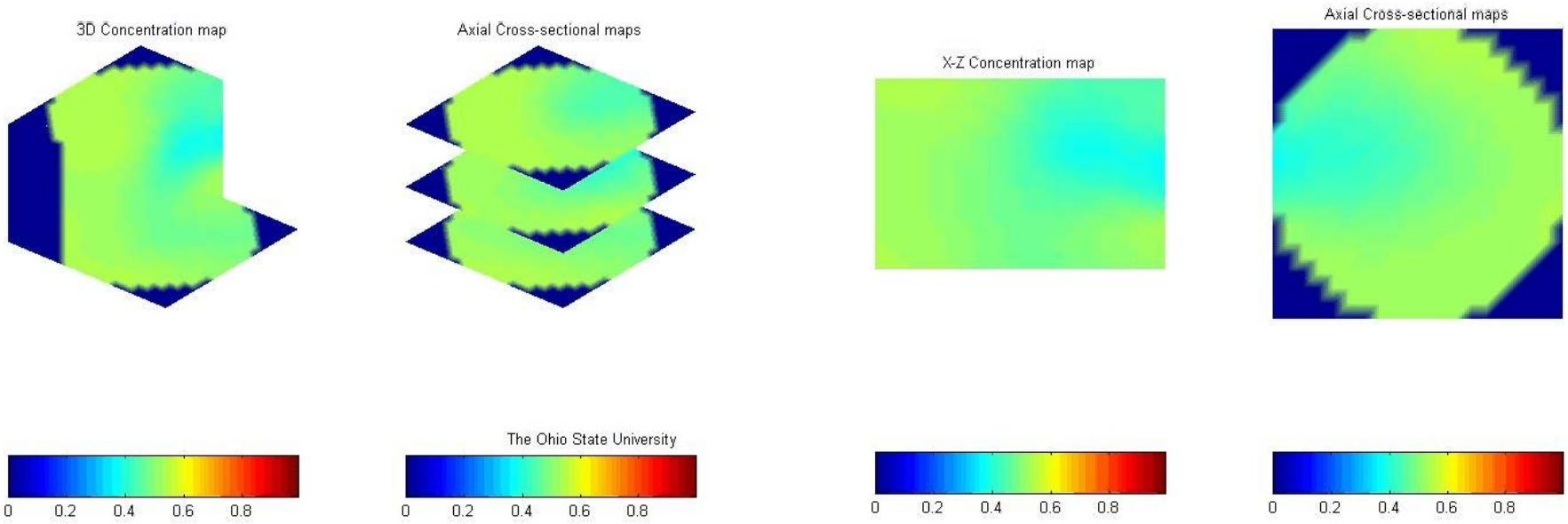

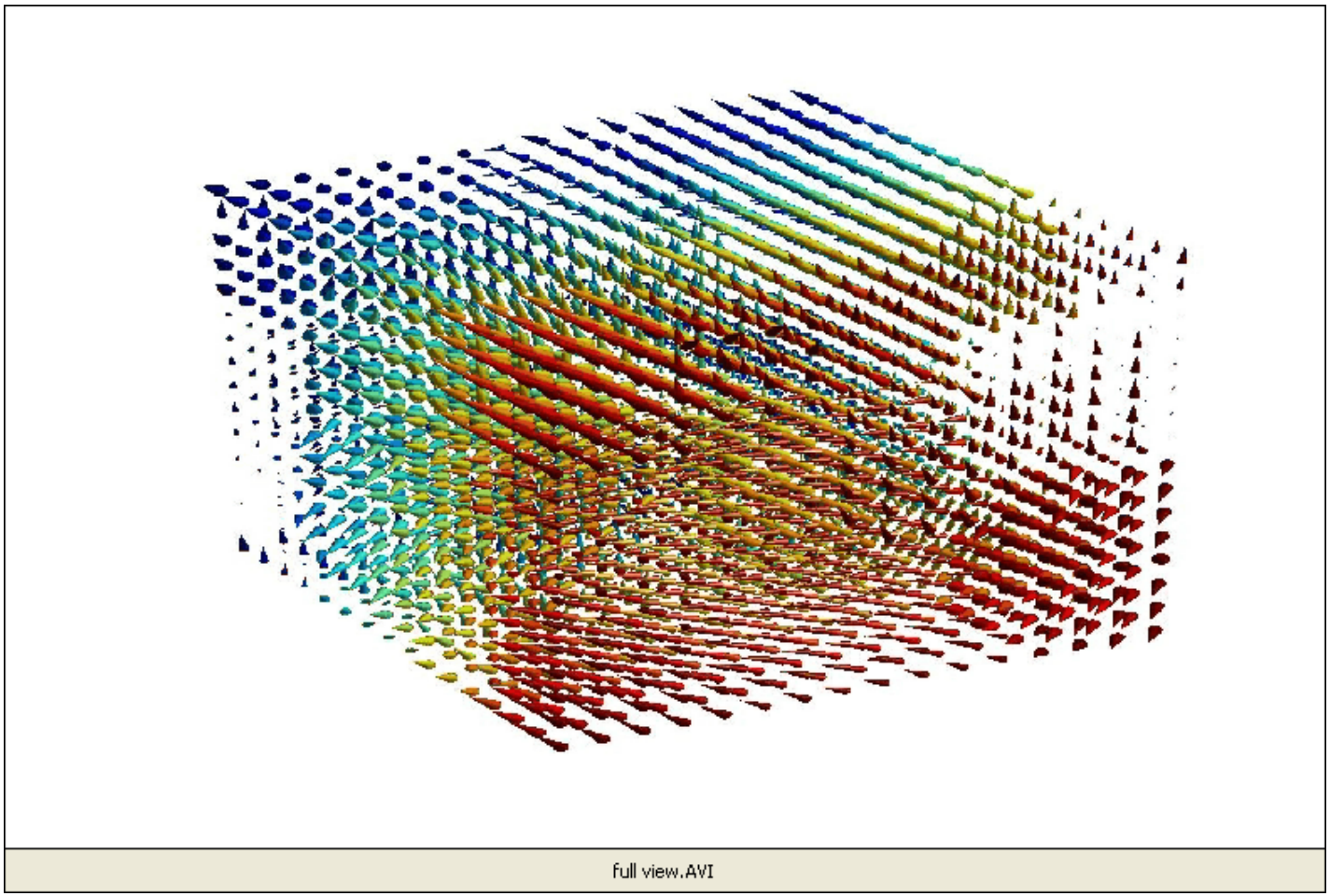
full view.AVI

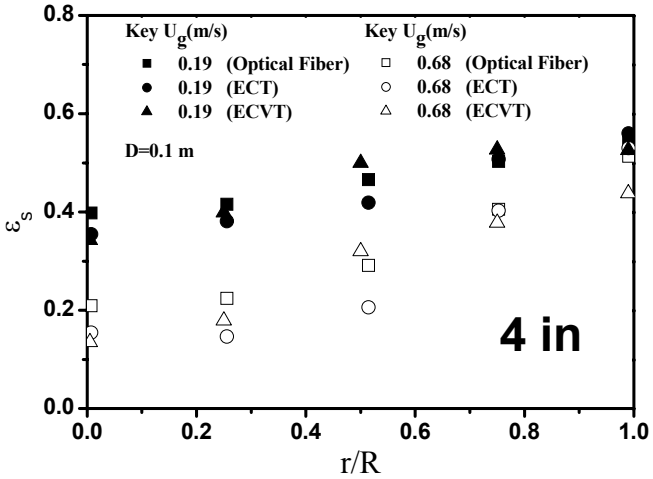

Radial profiles of time-averaged solids concentration in a 4-in gas-solid fluidized bed with FCC particles (d_p = 60 μm; ρ_p = 1400 kg/m^3) *obtained by ECVT, ECT and optical fiber probe*

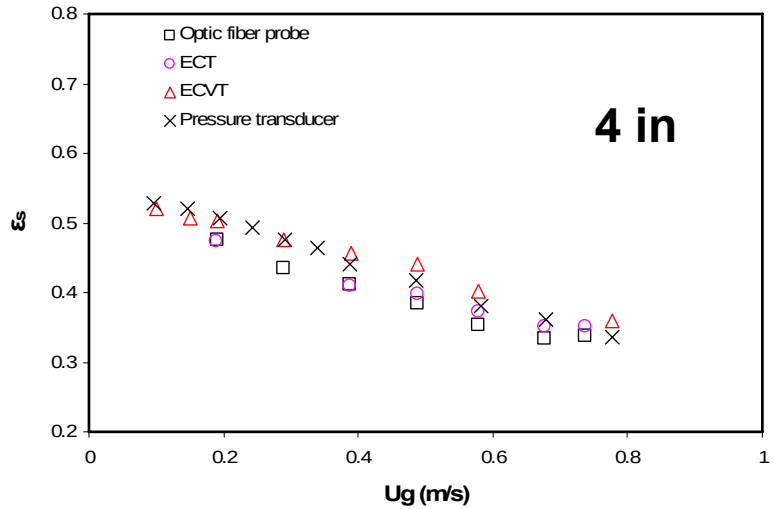

Comparison of the time-averaged cross-sectional solids concentrations obtained by *ECT* and *optical fiber probe* and the time-averaged volume solids concentration obtained by *ECVT* and *pressure transducer* for a 4-in gas-solid fluidized bed with FCC particles (d_p = 60 μm; ρ_p = 1400 kg/m^3)

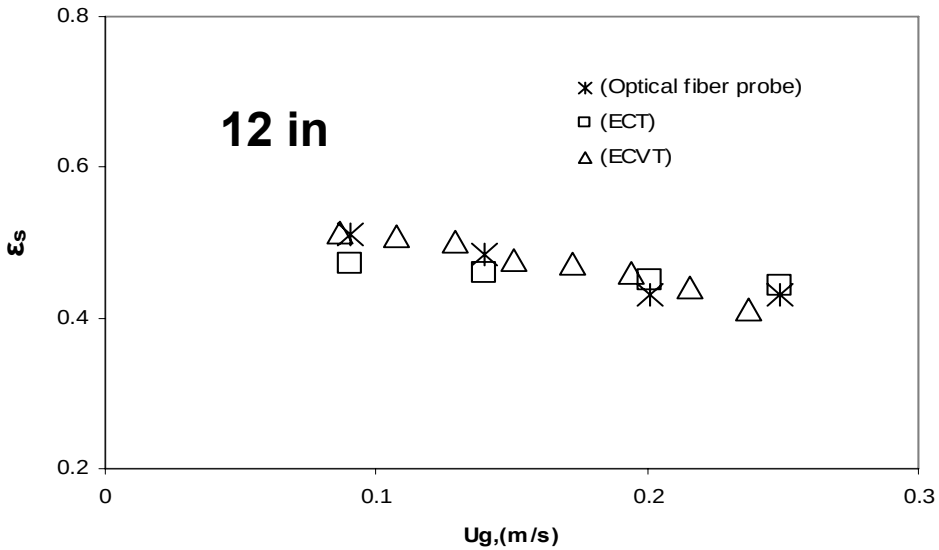

Comparison of the time-averaged cross-sectional solids concentrations obtained by the *ECT* and the *optical fiber probe* and the time-averaged volume solids concentration obtained by the *ECVT* for a 12-in gas-solid fluidized bed with FCC particles (d_p = 60 μm; ρ_p = 1400 kg/m^3)

Comparisons of Solids Fraction Measured by ECT and Optical Fiber Probe

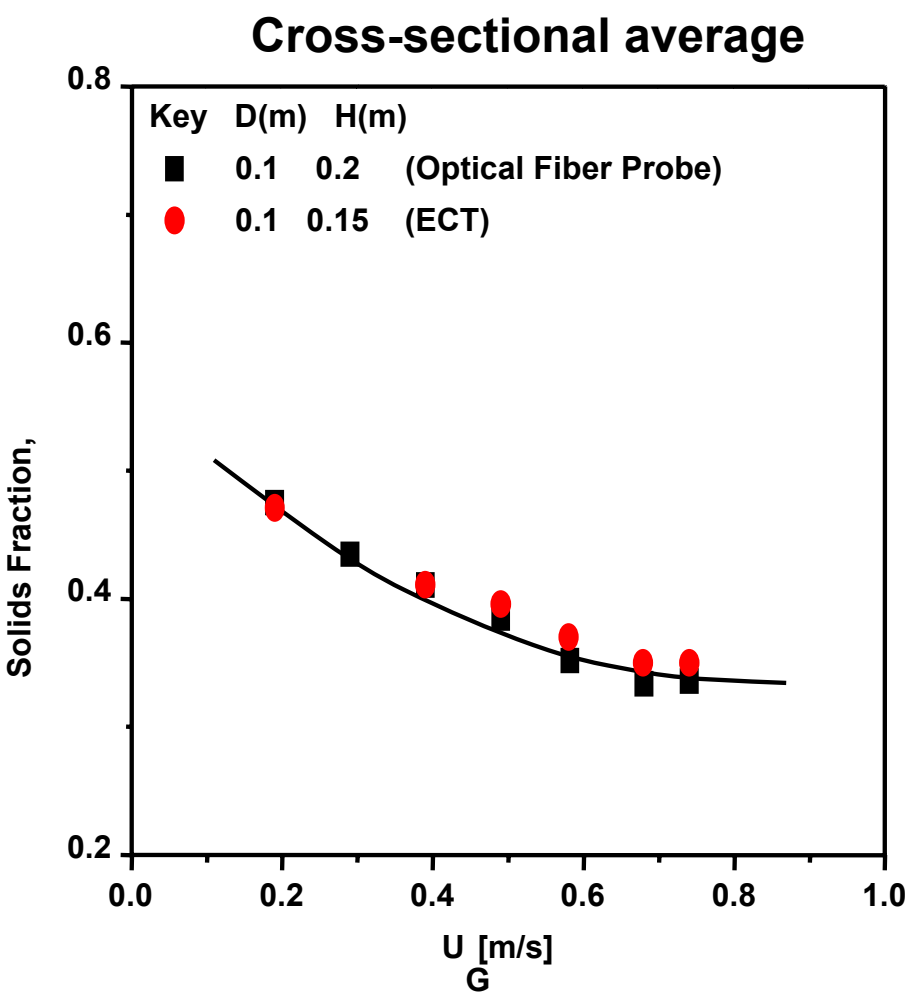

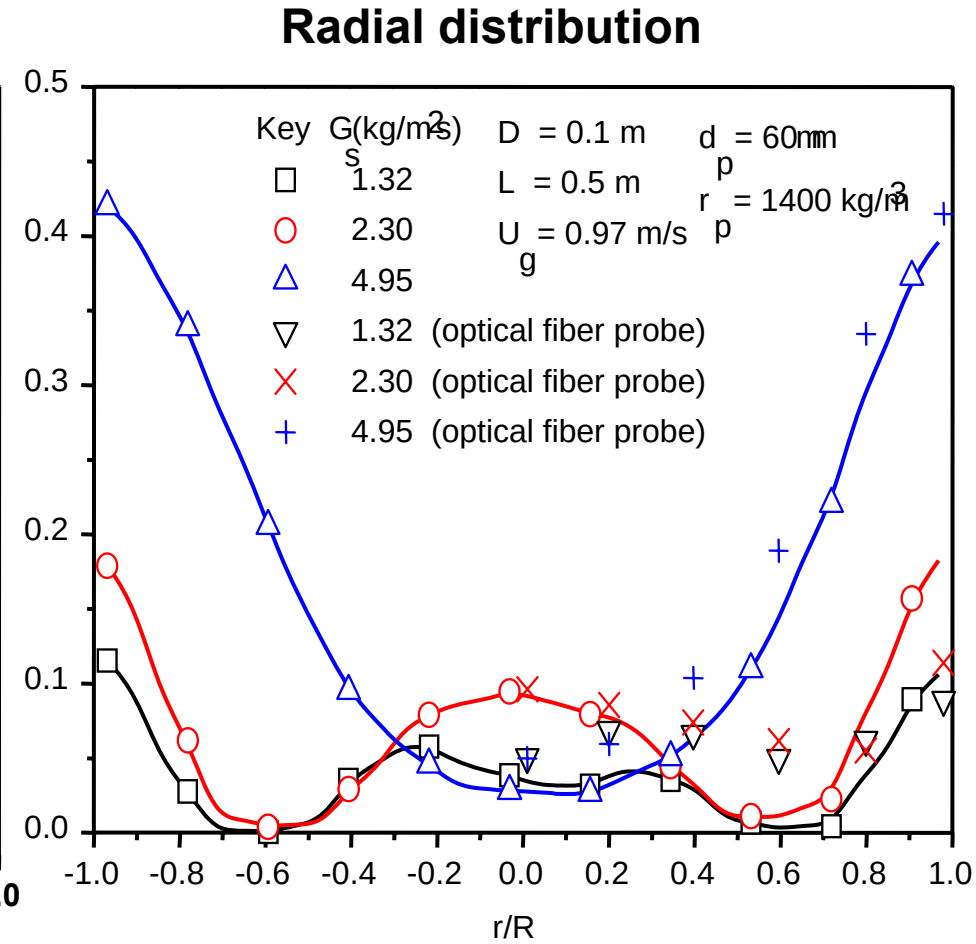

Electrical Capacitance Volume Tomography – Comparison with MRI

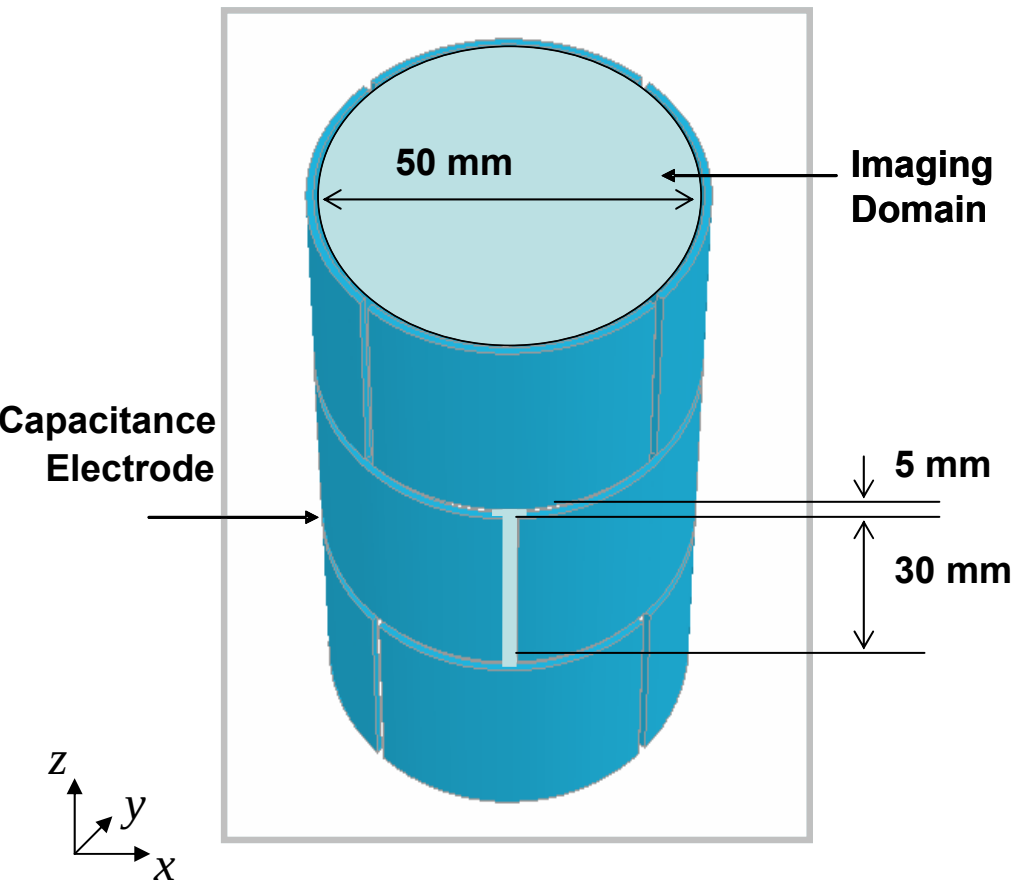

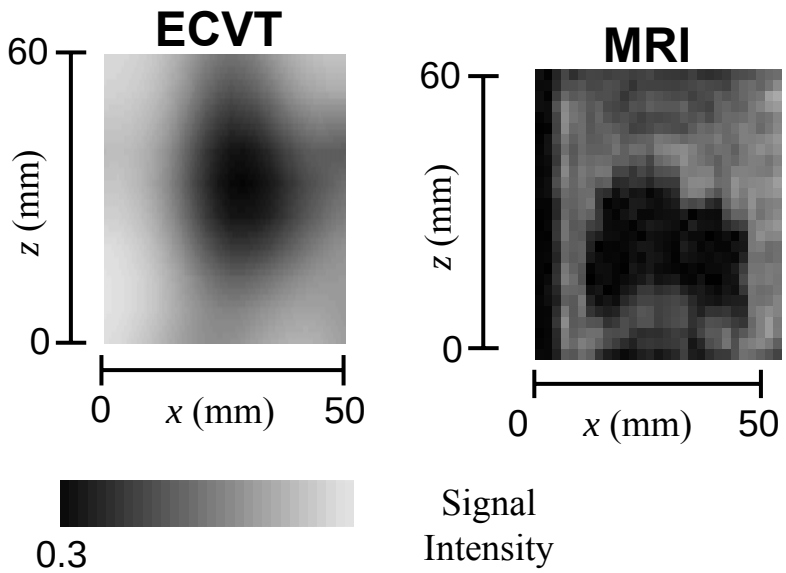

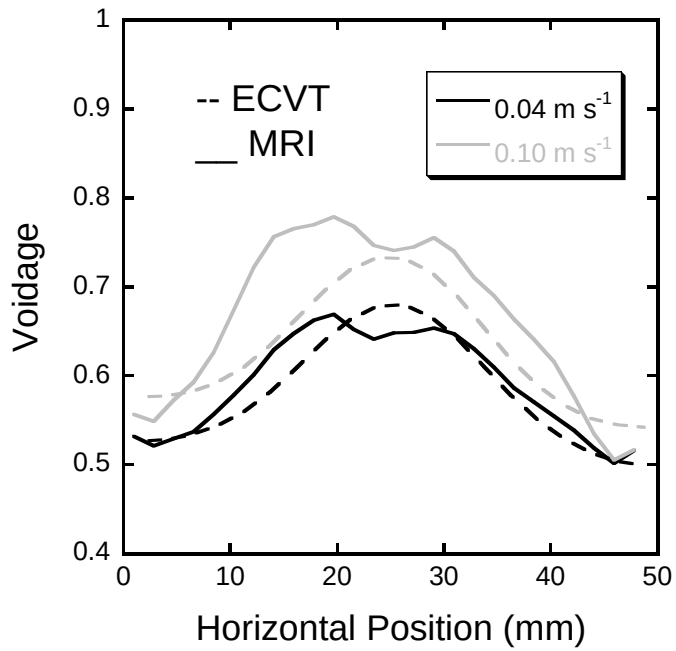

Work of **D.J. Holland[1], Q. Marashdeh[2], C.R. Müller[1], F. Wang[2], J.S. Dennis[1], L.-S. Fan[2], L.F. Gladden[1]**
[1]Cambridge University, [2]The Ohio State University

Electrical Capacitance Volume Tomography – Comparison with MRI

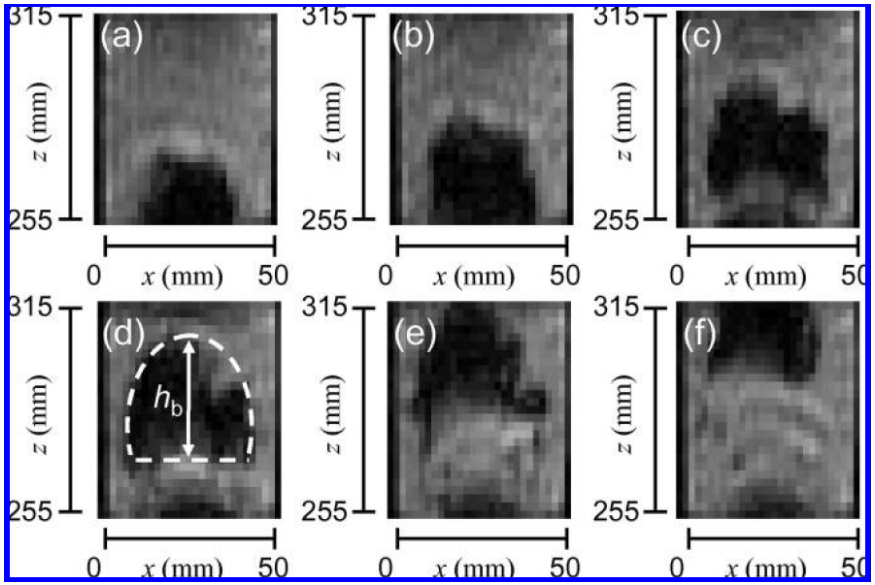

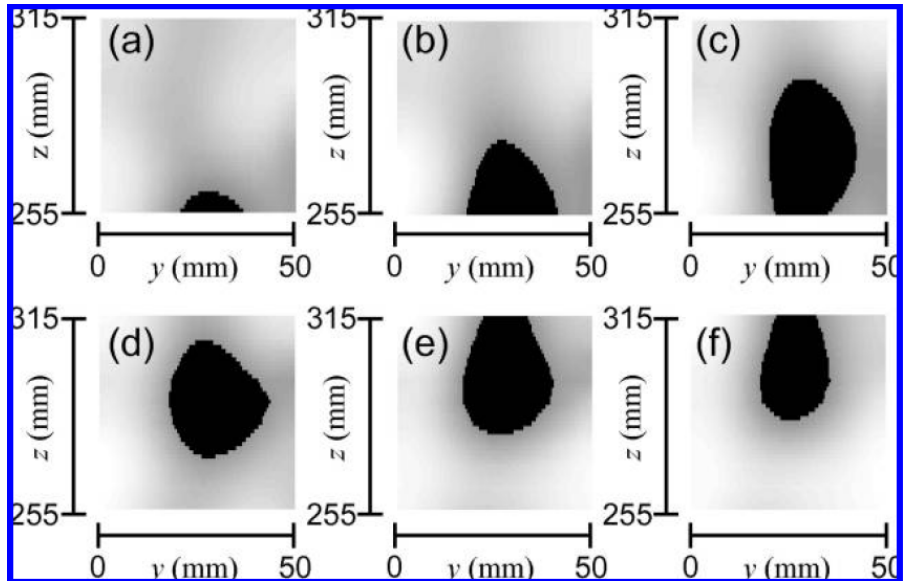

Superficial Gas Velocity: 0.04 m/s;
MRI: every frame (26 ms)
ECVT: every 2nd frame (25 ms)

Work of **D.J. Holland[1], Q. Marashdeh[2], C.R. Müller[1], F. Wang[2], J.S. Dennis[1], L.-S. Fan[2], L.F. Gladden[1]** [1]Cambridge University, [2]The Ohio State University

Electrical Capacitance Volume Tomography – Comparison with MRI

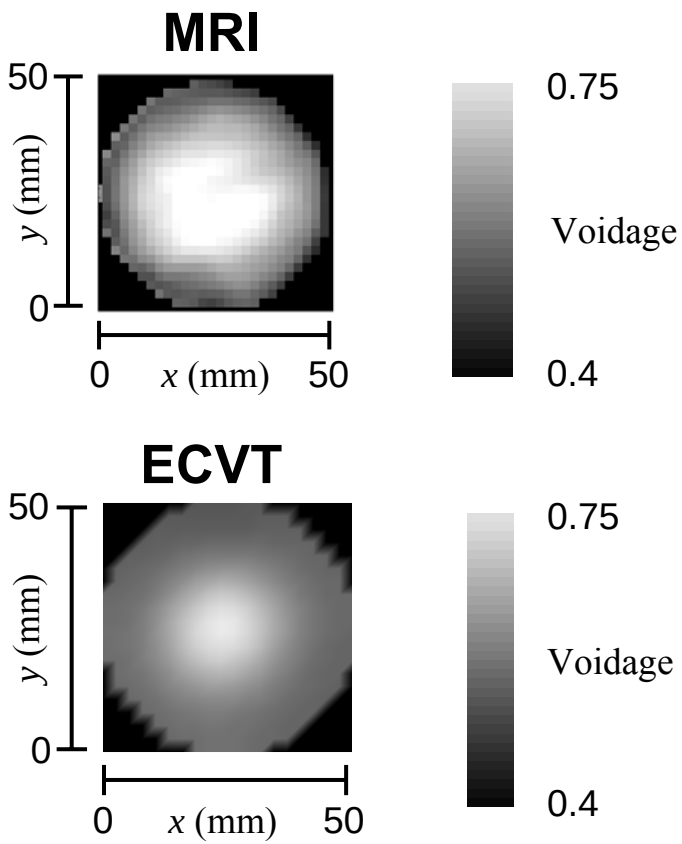

Superficial Gas Velocity: 0.104 m s-1

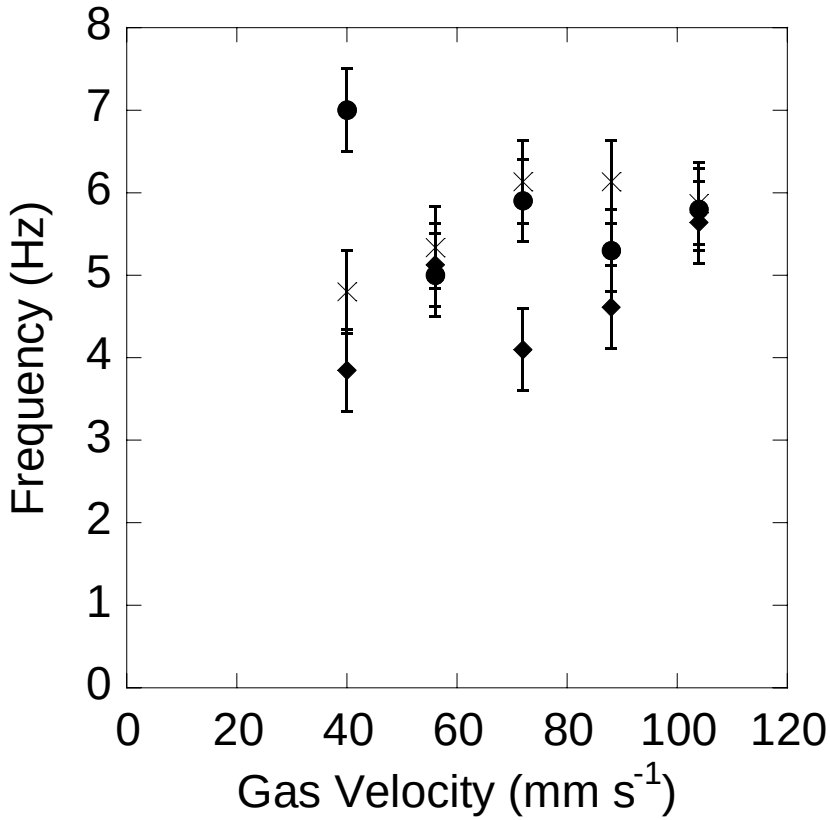

Bubble frequency calculated from the ECVT (×), 2D MR data (♦) and 1D MR data (●).

Work of **D.J. Holland[1], Q. Marashdeh[2], C.R. Müller[1], F. Wang[2], J.S. Dennis[1], L.-S. Fan[2], L.F. Gladden[1]**

[1]Cambridge University, [2]The Ohio State University

On-line ECVT and New Sensor Configurations

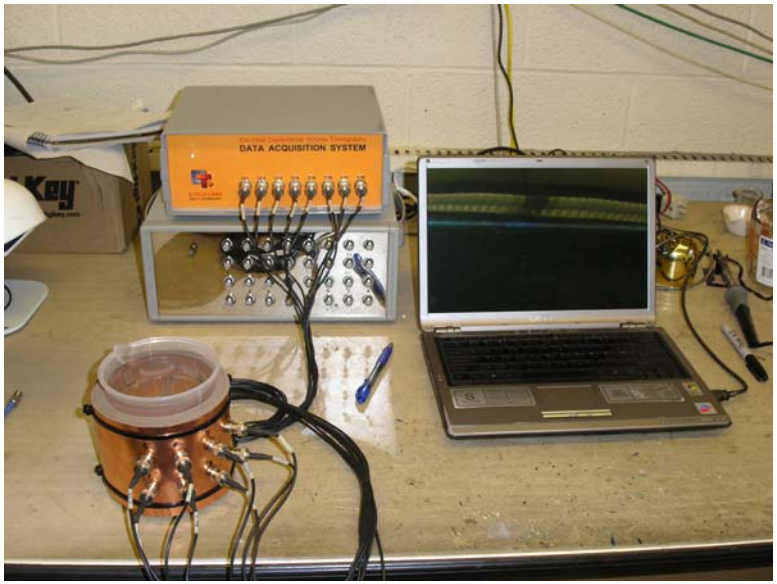

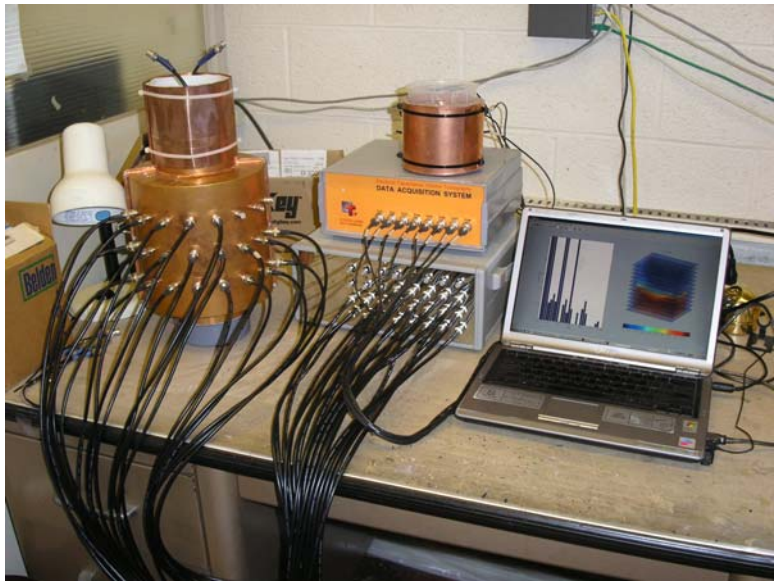

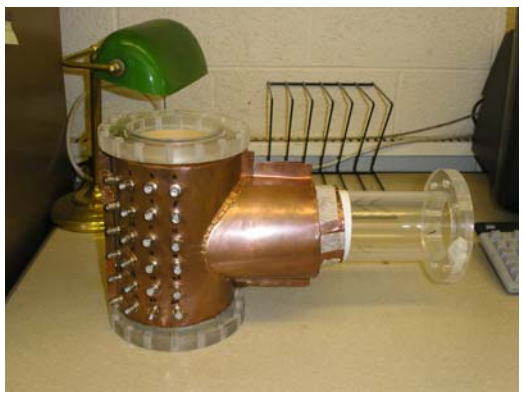

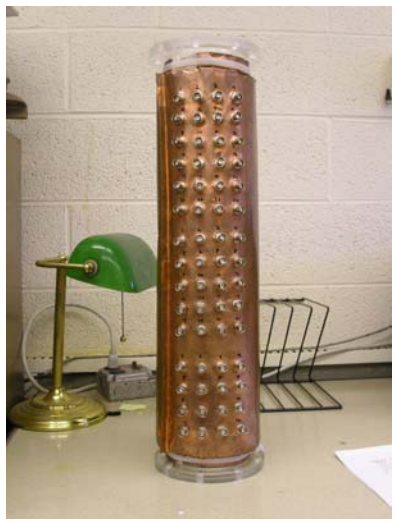

Electrical Capacitance Volume Tomography –
Sensor Design and Image Reconstruction Simulation in a Bend

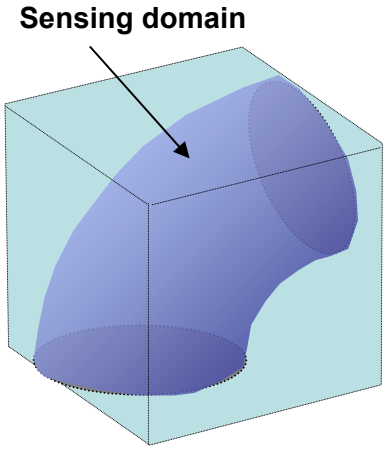

20X20X20 Voxels

(a)

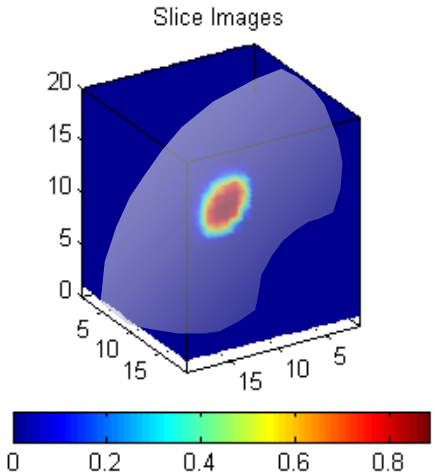

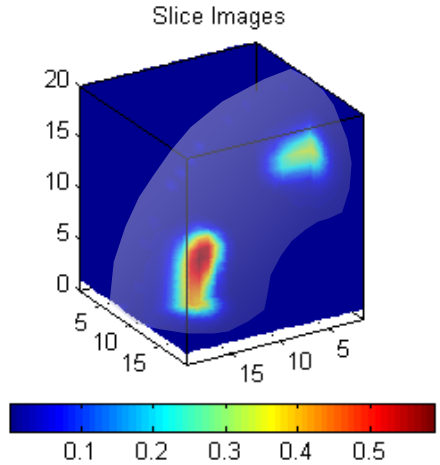

12-electrode sensor

(b)

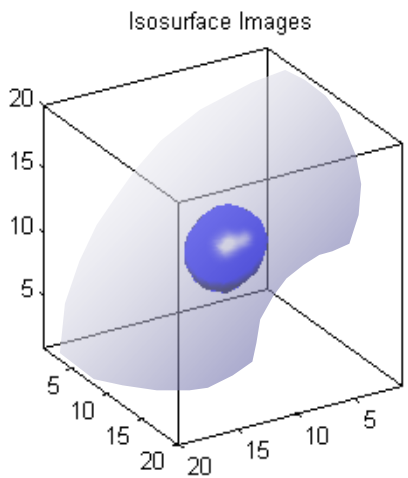

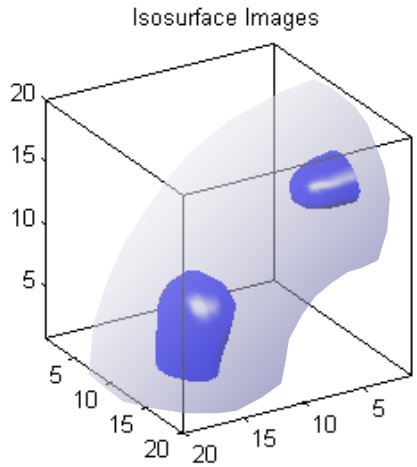

Work of **Q. Marashdeh[1]**, **W. Warsito[2]** and **L.-S. Fan[1]**
[1]The Ohio State University, [2]Ctech Labs.

Electrical Capacitance Volume Tomography - Commercial Usage, 60 inch ID Sensor

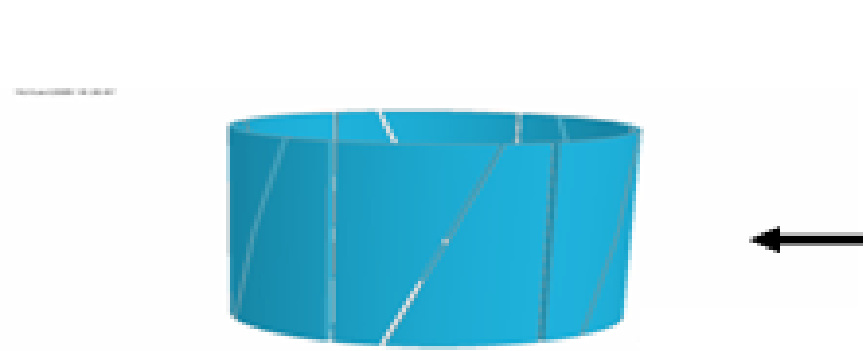

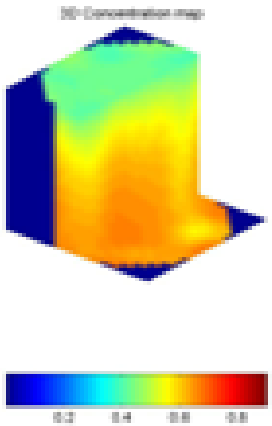

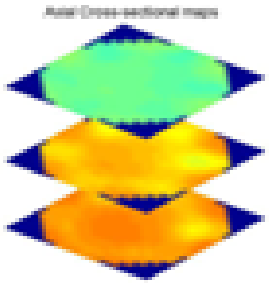

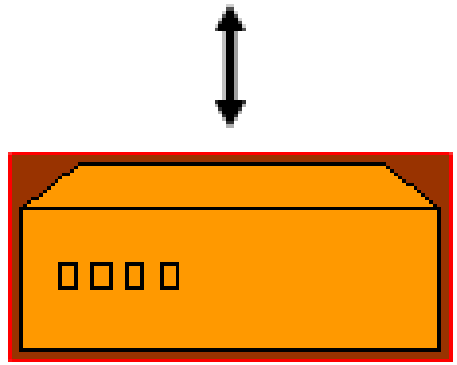

Acquisition System

Work of **Q. Marashdeh**[1], **W. Warsito**[2], **F. Wang**[1], and **L.-S. Fan**[1]
[1]The Ohio State University, [2]Ctech Labs.

Concluding Remarks

- The ECVT provides 3D real-time accurate images for multiphase flow fields with or without particle charges. The EST can map out particle charge distributions. The Multi-Modal Capacitance and Resistance measurements provide tomographic images of particle with conductive or dielectric properties.
- The robust neural network image reconstruction technique for the ECVT is extendible to EIT for medical imaging applications.
- The work on velocimetry applications is in progress

ACKNOWLEDGEMENT

- **Students and Research Associates:**

  Dr. W. Warsito, Dr. B. Du, Dr.A. Park, Dr. Q. Marashdeh, and F. Wang

- **Sponsors:**

  U. S. Department of Energy, Tech4Imanging, and industry